Probing the genetic code and impacts of mistranslation using $tRNA^{Ala}$ anticodon variants

Ecaterina Cozma[1], Megha Rao[1], Madison Dusick[1], Julie Genereaux[1], Ricard A. Rodriguez-Mias[2], Judit Villén[2], Christopher J. Brandl[1] and Matthew D. Berg[2]*

[1]Department of Biochemistry, The University of Western Ontario, London, Ontario N6A 5C1 Canada
[2]Department of Genome Sciences, University of Washington, Seattle, WA 98105, USA

*Corresponding author: Matthew Berg, Department of Genome Sciences, University of Washington, Seattle, WA 98105, USA Email: mattberg@uw.edu

Keywords: mistranslation, $tRNA^{Ala}$, genetic code, expanded decoding, tRNA biology

ABSTRACT

Transfer RNAs (tRNAs) maintain translational fidelity through accurate charging by their cognate aminoacyl-tRNA synthetase and codon:anticodon base pairing with the mRNA at the ribosome. Mistranslation occurs when an amino acid not specified by the genetic code is incorporated into a protein. Since alanyl-tRNA synthetase uniquely recognizes a G3:U70 base pair in $tRNA^{Ala}$ and the anticodon plays no role in charging, $tRNA^{Ala}$ variants with anticodon mutations have the potential to mis-incorporate alanine. Our goal was to characterize the phenotypic consequences of expressing all 60 $tRNA^{Ala}$ anticodon variants in *Saccharomyces cerevisiae*. Overall, 36 $tRNA^{Ala}$ anticodon variants decreased growth in single- or multi-copy. Using mass spectrometry, we observed mistranslation for 45 of 57 variants when on single-copy plasmids. Variants with G/C rich anticodons tend to have larger growth deficits and mistranslate at greater frequencies than A/U rich variants. There was a weak but statistically significant correlation between mistranslation and reduced growth. In most instances, synonymous anticodon variants impact growth differently. We suggest that this is explained by decoding specificity, which results in different $tRNA^{Ala}$ variants mistranslating unique sets of peptides and proteins. Since potential mistranslating tRNAs exist in humans, our analysis identifies features of $tRNA^{Ala}$ variants that influence their potential contribution to disease.

INTRODUCTION

Transfer RNAs (tRNAs) are adaptor molecules that decode the genetic message contained within mRNA into protein sequence during translation (1–4). Translational fidelity and proteome accuracy is maintained by tRNAs during two steps. First, tRNAs are recognized by their aminoacyl-tRNA synthetase (aaRS) and charged with the cognate amino acid. Second, accurate base pairing between the tRNA anticodon and mRNA codon during decoding at the ribosome ensures the correct amino acid is incorporated into the growing polypeptide chain (5–7). Errors at either step lead to mistranslation, the incorporation of an amino acid not specified by the genetic code. Mistranslation occurs naturally in all cells, with mis-incorporation events occurring once in every 10^4 to 10^5 codons (8–10). In addition, mistranslation frequency increases in response to environmental conditions (11–13) or in the presence of tRNA variants (14–17).

Aminoacyl-tRNA synthetases recognize their cognate tRNAs through individual bases or structural motifs within the tRNA called identity elements (18–20). For most tRNAs, the anticodon is the main identity element, providing a direct link between the genetic code and amino acid being incorporated. This is not the case for $tRNA^{Ala}$, $tRNA^{Ser}$ and $tRNA^{Leu}$, which are recognized by identity elements outside of the anticodon (20). Specifically, the alanyl-tRNA synthetase (AlaRS) recognizes a conserved G3:U70 base pair in the $tRNA^{Ala}$ acceptor stem (21–23). Similarly, the seryl- and leucyl-tRNA synthetases recognize a uniquely long variable arm in $tRNA^{Ser}$ and $tRNA^{Leu}$ positioned 3' of the anticodon stem (24–27). Consequently, anticodon mutations in $tRNA^{Ala}$, $tRNA^{Ser}$ or $tRNA^{Leu}$ can result in mis-incorporation of alanine, serine or leucine, respectively, at non-cognate codons (16, 17, 27, 28). Alanine mis-incorporation also arises through the insertion of a G3:U70 base pair in non-alanine tRNAs (14, 29–31).

Elevated levels of mistranslation from tRNA variants result in mis-made proteins across the proteome and proteotoxic stress. Protein quality control mechanisms allow cells to cope with mis-made proteins. These include the ubiquitin-proteasome system, autophagy, induction of the heat shock response and unfolded protein response, and the organization of protein aggregates into inclusion bodies (32). Ruan *et al.* demonstrated that *Escherichia coli* tolerate mistranslation of asparagine to aspartic acid at frequencies of ~ 10% (33) and we recently showed that *Saccharomyces cerevisiae* tolerate mistranslation of proline to serine at frequencies below 12% (34).

Cells also tolerate mistranslating tRNA variants by buffering their mis-incorporation potential with multiple copies of native, wild-type tRNA genes with identical or overlapping codon specificities. For example, *S. cerevisiae* contains 16 tRNAs genes that decode alanine codons, 11 with an AGC anticodon and 5 with a UGC anticodon. These two alanine isoacceptors decode the full set of four alanine codons (GCN) as the result of G:U wobble base pairing between base 34 and the third position of the codon and other extended pairing achieved through modification of base 34 (35, 36). In eukaryotic tRNAs, the latter involves modification of adenosine to inosine at position 34 to allow decoding of codons ending in A, U or C (37). Furthermore, uridine at position 34 is often modified to expand or restrict decoding potential (38, 39). Modification of bases outside the anticodon also affect decoding. For example, position 37, immediately 3' of the anticodon, is often modified to N^6-isopentenyladenosine and N^6-threonylcarbamoyladenosine for tRNAs that decode codons beginning in U or A, respectively (40). These modifications stabilize A:U Watson-Crick pairs in the first codon position. Overall, modifications ensure efficient decoding of all 61 sense codons.

With one or two mutations to the anticodon, $tRNA^{Ala}$ genes are theoretically capable of mis-incorporating alanine at any non-alanine codon. Mistranslation could increase genetic diversity and, on a longer time scale, lead to genetic code evolution. At the organism level, mistranslation caused by a $tRNA^{Ala}$ variant may result in proteotoxic stress and reduced fitness. To test the impact of different $tRNA^{Ala}$ variants on cells, we engineered a collection of $tRNA^{Ala}$ encoding genes with all 64 possible anticodons and individually measured their impact on growth and mistranslation frequency. Surprisingly, not all variants impact growth or mistranslate. The impact of a variant was primarily dictated by the anticodon, as opposed to the amino acid substitution being made. Specifically, G/C richness of the anticodon and base identity at position 34 were the predominant features influencing mistranslation frequency by the variant, whereas cellular impact was influenced by mistranslation frequency and the specificity of decoding. As human genomes contain tRNA anticodon variants with the potential to mistranslate (41), our results indicate that the impact of human $tRNA^{Ala}$ anticodon variants will depend on the specific anticodon of the tRNA variant. In addition, the mistranslating tRNAs generated here have applications in synthetic biology for making statistical proteins and proteomes (42, 43).

MATERIALS AND METHODS

Yeast strains and growth

Wild type haploid yeast strains are derivatives of BY4742 (***MATα his3Δ1 leu2Δ0 lys2Δ0 ura3Δ0***) (44). The haploid strain CY8652 (***MATα his3Δ1 leu2Δ0 lys2Δ0 ura3Δ0 tTA*-URA3)*** containing the tet "off" activator (tTA*) marked with *URA3* was derived from R1158 (45) after crossing with BY4741 and sporulation.

Yeast strains were grown at 30°C in yeast peptone medium or in synthetic medium supplemented with nitrogenous bases and amino acids containing 2% glucose. Transformations were performed using the lithium acetate method as previously described (46).

Growth assays

Inducible $tRNA^{Ala}$ anticodon variants. Yeast strain CY8652 constitutively expressing the TetR-VP16 protein and containing a *LEU2* plasmid expressing either a control $tRNA^{Ala}_{GGC(Ala)}$ decoding alanine codons or the anticodon variants were grown to saturation in medium lacking uracil and leucine without doxycycline. Strains were diluted to OD_{600} of 0.1 in the same medium containing 0, 0.01 or 1.0 µg/mL of doxycycline and grown for 24 hours at 30°C with agitation. OD_{600} was measured every 15 minutes for 24 hours in a BioTek Epoch 2 microplate spectrophotometer. Doubling time was calculated using the R package "growthcurver" (47). Doubling times were normalized to the wild-type strain grown at the respective doxycycline concentration. Each strain was assayed in triplicate.

2µ $tRNA^{Ala}$ anticodon variant derivatives. Yeast strain BY4742 was transformed with 1.0 µg of plasmid expressing the control $tRNA^{Ala}_{CGC(Ala)}$ or anticodon variant tRNAs and plated onto minimal medium lacking uracil. Plates were imaged after 2 days of growth and quantified using the ImageJ (48) "Watershed" package.

DNA constructs

The construct encoding the $tRNA^{Ala}$ variants was synthesized as a GeneString fragment (ThermoFisher) containing a random mix of each nucleotide at anticodon positions 34, 35 and 36 and the $tRNA^{Ala}$ gene was flanked by approximately 300 base pairs of up- and downstream sequence from *SUP17.* The synthetic gene fragment was cloned as a *Hin*dIII/*Not*I fragment into pCB4699, a *LEU2* centromeric plasmid (YCplac111) containing a tetracycline regulated promoter downstream of the tRNA gene as previously described (34). For variants that were not selected out of the randomized anticodon pool, constructs expressing these $tRNA^{Ala}$ variants were engineered via two-step PCR reactions. To reduce the number of primers needed, mismatched primer sets were used to generate two variants from a single PCR reaction. PCR fragments were subcloned into pGEM-Teasy (Promega) and then moved as *Hin*dIII/*Not*I fragments into pCB4699. The sequences of all 64 $tRNA^{Ala}$ anticodon variants generated and plasmid numbers are listed in Supplementary Table 1. The cloning approach and primers used to generate each variant (if applicable) are listed in Supplementary Table 2.

Multicopy plasmid expressing $tRNA^{Ala}$ variants were made by cloning *Hin*dIII/*Eco*RI fragments containing each tRNA variant into YEplac195. Plasmid numbers are listed in Supplemental Table 3.

Mass spectrometry

Strains were grown overnight in medium lacking leucine and uracil. Cultures were diluted to OD_{600} of 0.01 in the same medium containing 1.0 µg/mL doxycycline except for the strain expressing $tRNA^{Ala}_{CGG(Pro)}$ which was diluted to OD_{600} of 0.1. Cultures were harvested by washing once in 1x yeast nitrogen base and frozen in liquid nitrogen when they reached an OD_{600} between 0.8–1.0, except for $tRNA^{Ala}_{GCC(Gly)}$ which due to its slow growth was harvested 36 hours after dilution at OD_{600} ~ 0.4.

Cells were lysed by bead-beating with 0.5 mm glass beads at 4°C in urea lysis buffer (8 M urea, 50 mM Tris pH 8.2, 75 mM NaCl). Lysates were cleared by centrifugation at 21,000 x g for 10 minutes at 4°C and protein concentration was determined by bicinchoninic acid assay (Pierce, ThermoFisher Scientific). Proteins were reduced with 5 mM dithiothreitol for 30 minutes at 55°C, alkylated with 15 mM iodoacetamide for 30 minutes at room temperature in the dark and the alkylation was quenched with an additional 5 mM dithiothreitol for 30 minutes at room temperature. For each sample, 50 µg of protein was diluted 4-fold with 50 mM Tris pH 8.9 and digested for 4 hours at 37°C with 1.0 µg LysC (Wako Chemicals). Digestions were acidified to pH 2 with trifluoroacetic acid and desalted over Empore C18 stage tips (49).

For strains containing $tRNA^{Ala}_{UUU(Lys)}$ and $tRNA^{Ala}_{CUU(Lys)}$ and the corresponding control strain containing $tRNA^{Ala}_{GCC(Ala)}$, samples were lysed as above in 4 M guanidine hydrochloride, 100 mM triethylammonium bicarbonate pH 8.0. Samples were prepared as above, except after quenching the alkylation reaction, 100 µg of protein was acetylated with 200 µg of Sulfo-NHS-acetate (Pierce, ThermoFisher Scientific) for 1 hr at room temperature. Robotic purification and digestion of proteins into peptides was performed on the Kingfisher Flex (ThermoFisher Scientific) using trypsin and the R2-P1 method described by Leutert *et al.* (50). Digestions were acidified and desalted as above. Peptides were resuspended in 200 mM EPPS pH 9.5 with 5% hydroxylamine and incubated for 5 hrs at room temperature to reduce acetylation on serine, threonine and tyrosine residues before peptides were desalted again.

Peptide samples were resuspended in 4% acetonitrile, 3% formic acid and subjected to liquid chromatography coupled to tandem mass spectrometry on a tribrid quadrupole orbitrap mass spectrometer (Orbitrap Eclipse; ThermoFisher Scientific). Samples were loaded onto a 100 µm ID x 3 cm precolumn packed with Reprosil C18 3 µm beads (Dr. Maisch GmbH) and separated by reverse-phase chromatography on a 100 µm ID x 30 cm analytical column packed with Reprosil C18 1.9 µm beads (Dr. Maisch GmbH) housed into a column heater set at 50°C. Peptides were separated using a gradient of 7-50% acetonitrile in 0.125% formic acid delivered at 400 nL/min over 95 minutes, with a total 120-min acquisition time. The mass spectrometer was operated in data-dependent acquisition mode with a defined cycle time of 3 seconds. For each cycle, one full mass spectrometry scan was acquired from 350 to 1200 m/z at 120,000 resolution with a fill target of 3E6 ions and automated calculation of injection time. The most abundant ions from the full MS scan were selected for fragmentation using 1.6 m/z precursor isolation window and beam-type collisional-activation dissociation (HCD) with 30% normalized collision energy. MS/MS spectra were acquired at 15,000 resolution by setting the AGC target to standard and injection time to automated mode. Fragmented precursors were dynamically excluded from selection for 60 seconds.

MS/MS spectra were searched against the *S. cerevisiae* protein sequence database (downloaded from the Saccharomyces Genome Database resource in 2014) using Comet (release 2015.01) (51). The precursor mass tolerance was set to 20 ppm. Constant modification of cysteine carbamidomethylation (57.0125 Da) and variable modification of methionine oxidation (15.9949 Da) was used for all searches. For samples containing $tRNA^{Ala}_{UUU(Lys)}$, $tRNA^{Ala}_{CUU(Lys)}$ and the corresponding control samples, variable modification of lysine acetylation (42.0105 Da) was included. A variable modification of each amino acid to alanine was used for the respective searches. A maximum of 3 of each variable modification was allowed per peptide. Search results were filtered to a 1% false discovery rate at the peptide spectrum match level using Percolator (52). Mistranslation frequency was calculated from the unique mistranslated peptides for which the non-mistranslated sibling peptide was also observed. The frequency is defined as the counts of unique mistranslated peptides, where alanine had been mis-incorporated, divided by the counts of all peptides containing the wild-type amino acid and expressed as a percentage. At the codon level, mistranslation frequency was determined using a custom Perl script (Supplemental File 1) considering only peptides with one possible substitution event to allow for accurate localization of the mistranslation event and identification of the codon being mistranslated.

The raw mass spectrometry data have been deposited to the ProteomeXchange Consortium via the PRIDE (53) partner repository with the dataset identifier PXD038242 and an annotated list of the file names can be found in Supplemental Table S4.

Factors used to correlate mistranslation frequency and growth

Linear regression was performed between the following factors and mistranslation frequency for each $tRNA^{Ala}$ variant: wild-type tRNA gene copy number (54, 55), ribosome residence time at each codon (56) and the Turner values describing codon:anticodon binding energetics (57, 58). The following factors were correlated using multiple linear regression with the relative growth impact of each variant as the dependent variable: mistranslation frequency, amino acid polarity requirement (PR score) (59), BLOSUM substitution score (60), Kyte-Doolittle hydropathy index (61), yeast whole genome codon usage frequency (https://www.genscript.com/tools/codon-frequency-table) and codon usage in top 30 expressed yeast proteins (62, 63). SIFT scores for all possible substitutions to alanine in the yeast proteome were downloaded from the mutfunc resource (64, 65). For each codon, the number of predicted deleterious substitutions (SIFT

prediction score < 0.05) was determined. A weighted SIFT score was calculated for each $tRNA^{Ala}$ variant by multiplying the number of possible deleterious substitutions at a specific codon by the mistranslation frequency at that codon. For $tRNA^{Ala}$ variants that mistranslate at multiple codons, the weighted SIFT score for each codon was summed.

Statistical analyses

Statistical analyses were performed using R studio 1.4.1717. Representative code for all analyses can be found in Supplemental File 2. Welch's *t*-test was used to compare doubling times of strains containing $tRNA^{Ala}$ anticodon variants to the control $tRNA^{Ala}_{GGC(Ala)}$ strain and corrected for multiple tests using the Benjamini-Hochberg method. Wilcoxon rank sum test was used to compare median colony size of strains transformed with $tRNA^{Ala}$ anticodon variants on multicopy plasmids relative to the control $tRNA^{Ala}_{CGC(Ala)}$ and corrected for multiple tests using the Bonferroni method. Welch's *t*-test was used to compare the mistranslation frequency measured for strains containing $tRNA^{Ala}$ anticodon variants to the control $tRNA^{Ala}_{GGC(Ala)}$ strain and corrected for multiple tests using the Benjamini-Hochberg method. Simple linear regression was used to correlate number of tRNA genes, ribosome residence time and turner energy for each codon with mistranslation frequency and Pearson's R^2 was determined for each correlation. Multiple linear regression was used to correlate mistranslation frequency, amino acid polarity requirement (PR score), BLOSUM substitution score, Kyte-Doolittle hydropathy index, yeast whole genome codon usage frequency and codon usage in top 30 expressed yeast proteins with impact on growth. Independent variables with *p*-values less than 0.05 after Bonferroni multiple test correction were considered to contribute to growth impact of each $tRNA^{Ala}$ anticodon variant.

RESULTS

The anticodon determines the phenotypic impact of tRNA^{Ala} variants

To investigate the impact of tRNA^{Ala} anticodon variants on yeast growth, we engineered a collection of plasmids expressing the 64 possible tRNA^{Ala} anticodon derivatives (Figure 1A, Table S1). A tetracycline inducible system (34) was used to regulate tRNA expression and control mistranslation-associated toxicity (Figure 1B). In the absence of the tetracycline analog doxycycline, tRNA expression is repressed. When doxycycline is added to the growth media, the tRNA variant is expressed in a titratable manner. Since we previously found that regulation of this system was improved with tRNA^{Ser} *SUP17* flanking sequence (34), the tRNA^{Ala} encoding gene was positioned precisely into the *SUP17* locus (Figure S1).

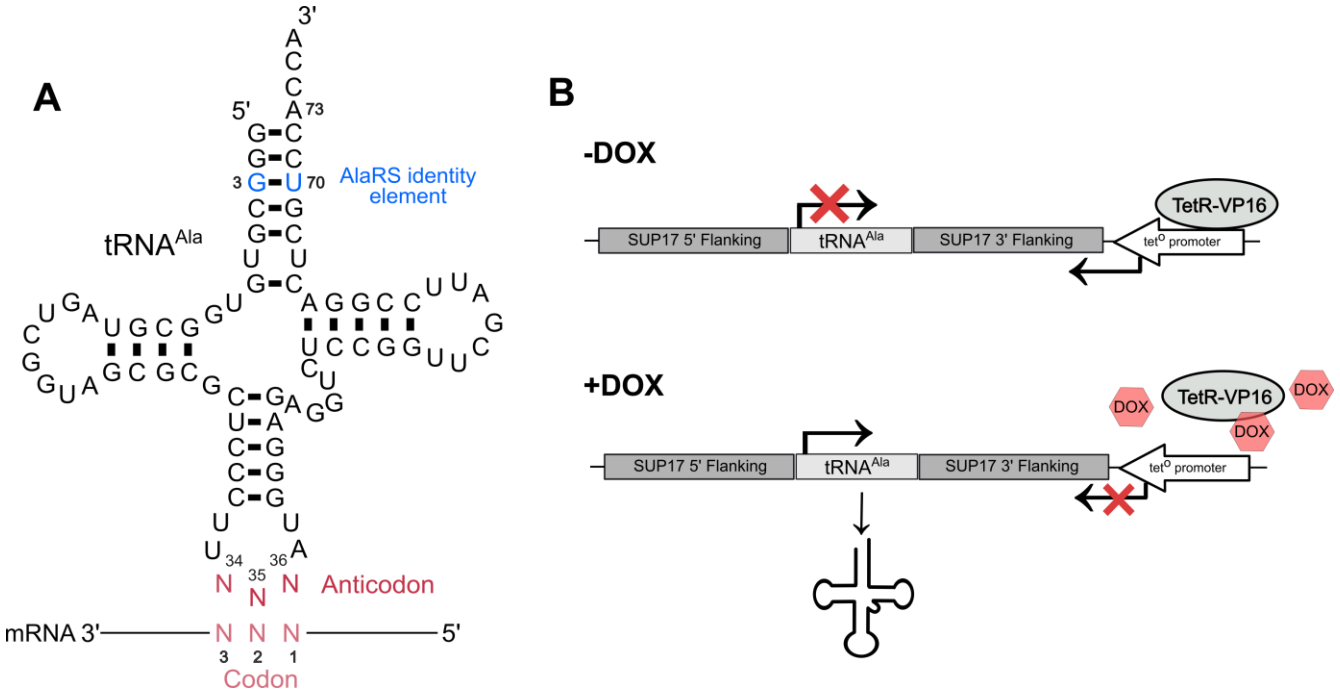

Figure 1. Schematic of tRNA^{Ala} containing a degenerate anticodon and the tetracycline inducible tRNA expression system. (A) The structure of tRNA^{Ala} with a degenerate anticodon. Bases colored in blue represent the G3:U70 base pair required for recognition and charging by AlaRS. The anticodon is shown in red. **(B)** tRNA^{Ala} in the tetracycline inducible system used to regulate tRNA^{Ala} anticodon variant expression flanked by up- and downstream *SUP17* sequence. In the absence of the tetracycline analog doxycycline, the tet^{O} promoter is bound by the TetR-VP16 transcriptional activator which represses tRNA expression by driving RNA polymerase II expression across the tRNA gene. In the presence of doxycycline, TetR-VP16 binds doxycycline and dissociates from the promoter allowing the tRNA to be transcribed by RNA polymerase III.

Plasmids containing one of 64 $tRNA^{Ala}$ anticodon variants were transformed into a yeast strain constitutively expressing Tet-VP16 (CY8652) (34). Transformants were isolated and their growth characterized in liquid minimal media containing 0, 0.01 and 1.0 µg/mL doxycycline. Growth curves were performed in biological triplicate for each strain at 30°C over 24 hours. Figure 2A shows representative growth curves for strains containing the control $tRNA^{Ala}_{GGC(Ala)}$ and variants $tRNA^{Ala}_{CAU(Met)}$, $tRNA^{Ala}_{GAA(Phe)}$ and $tRNA^{Ala}_{AGG(Pro)}$, which show minimal, intermediate and high impact on growth, respectively. As an example, $tRNA^{Ala}_{AGG(Pro)}$, reduces growth to 47% of the strain containing the control $tRNA^{Ala}_{GGC(Ala)}$ at 1.0 µg/mL doxycycline. As expected, growth impact was less severe at lower doxycycline concentrations for $tRNA^{Ala}_{GAA(Phe)}$ and $tRNA^{Ala}_{AGG(Pro)}$. Growth of the control $tRNA^{Ala}_{GGC(Ala)}$ and $tRNA^{Ala}_{CAU(Met)}$ was unchanged at all doxycycline concentrations.

The relative growth of each strain containing one of 64 possible $tRNA^{Ala}$ variants in medium with 1.0 µg/mL doxycycline is shown in Figure 2B and relative growth at all three doxycycline concentrations is shown in Figure S2. Of the 60 variants with non-alanine anticodons, 25 significantly decreased growth compared to the wild-type $tRNA^{Ala}$ (Table S7). For variants that significantly decreased growth, we observed a range of relative growth rates indicating that $tRNA^{Ala}$ variants with anticodons decoding the 19 non-alanine amino acids have diverse impacts. For example, G/C rich variants $tRNA^{Ala}_{CGG(Pro)}$, $tRNA^{Ala}_{GAC(Val)}$ $tRNA^{Ala}_{GCC(Gly)}$ and $tRNA^{Ala}_{CAG(Leu)}$ resulted in the greatest growth reduction. A moderate growth reduction was observed for variants encoding $tRNA^{Ala}_{GAA(Phe)}$, $tRNA^{Ala}_{GUG(His)}$, $tRNA^{Ala}_{GGA(Ser)}$. Variants that had no growth reduction include the A/U rich variants $tRNA^{Ala}_{AAA(Phe)}$, $tRNA^{Ala}_{AAU(Ile)}$, $tRNA^{Ala}_{UAU(Ile)}$, $tRNA^{Ala}_{UUU(Lys)}$, and $tRNA^{Ala}_{AUU(Asn)}$ as well as the variants decoding all three stop codons. In addition, different growth impacts were observed for variants decoding synonymous codons. For example, $tRNA^{Ala}_{GGU(Thr)}$ reduced growth to 61% of the wild-type, whereas the other three threonine decoding variants had a minimal effect.

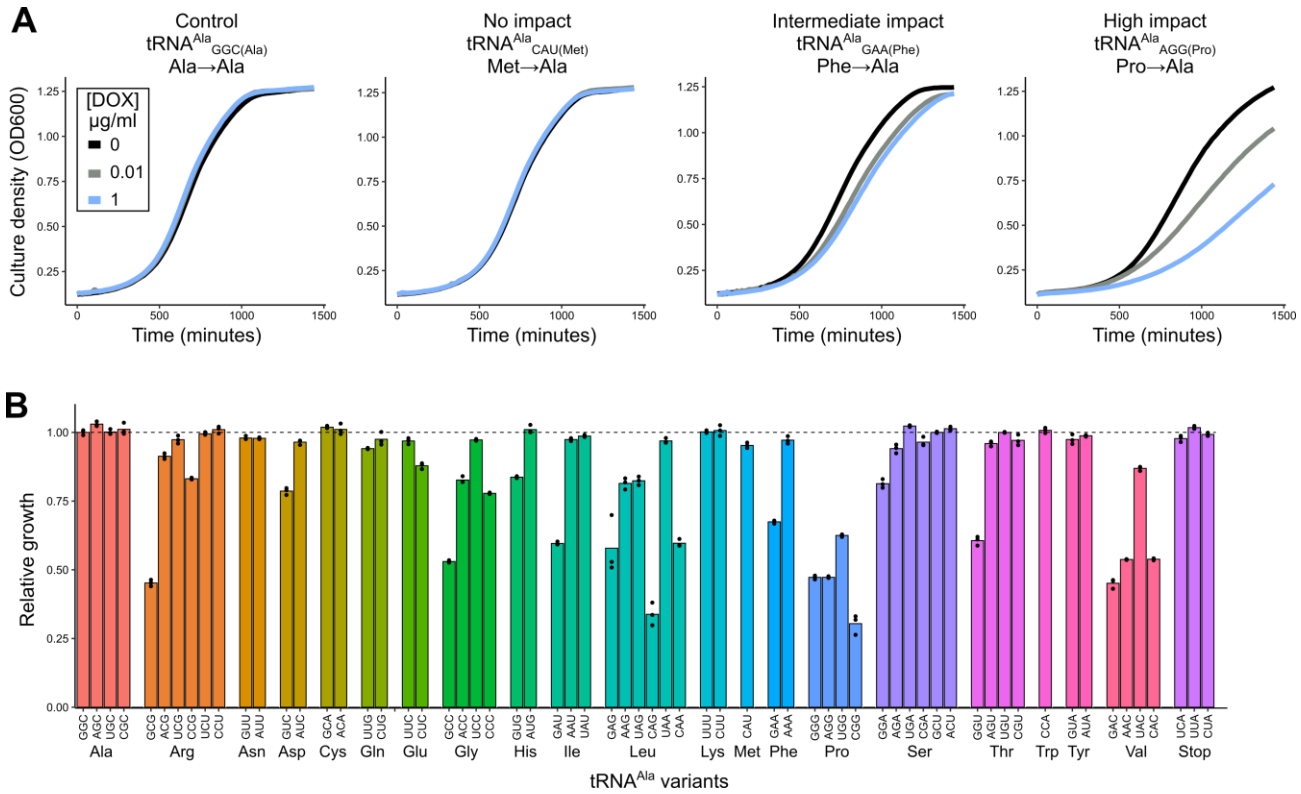

Figure 2. Impact of tRNA^{Ala} anticodon variants on yeast growth. (A) Representative growth curves of yeast strain CY8652 containing a plasmid with a control tRNA$^{Ala}_{GGC(Ala)}$ variant, a tRNA$^{Ala}_{CAU(Met)}$ variant with no growth effect, a tRNA$^{Ala}_{GAA(Phe)}$ variant with intermediate growth impact or a tRNA$^{Ala}_{AGG(Pro)}$ variant with a severe growth impact. Black, grey and blue lines represent strains grown in media containing 0, 0.01 and 1.0 µg/mL doxycycline, respectively. **(B)** Relative growth of tRNA^{Ala} anticodon variants in medium containing 1.0 µg/mL doxycycline was calculated by multiplying the inverse of each variant's doubling time by the average doubling time of the tRNA$^{Ala}_{GGC(Ala)}$ control (for raw data and statistical comparisons see Table S6 and S7). Cultures were grown for 48 hours at 30°C in medium lacking uracil and leucine, diluted to an OD_{600} of 0.1 in the same medium with 1.0 µg/mL doxycycline and grown for 24 hours at 30°C with agitation. OD_{600} was measured at 15-minute intervals and doubling time was quantified with the 'growthcurver' R package. Each point represents one biological replicate (n = 3).

Increasing tRNA^{Ala} anticodon variant copy number reveals growth impact

Thirty-nine variants did not show statistically slower growth when compared to the control tRNA$^{Ala}_{GGC(Ala)}$ in single copy. Since each tRNA^{Ala} anticodon variant competes with the native tRNA species for decoding, we tested if increasing copy number would uncover a growth phenotype. We cloned a subset of the tRNA^{Ala} anticodon variants into a 2µ multicopy plasmid. The wild-type BY4742 strain was transformed with these plasmids and transformant colony size quantified relative to a control transformation of tRNA$^{Ala}_{CGC(Ala)}$ on a multicopy plasmid (Figure 3, Figure S3, Table S8). We chose to quantify colony size after transformation to minimize the number of passages and selection pressure towards lower copy of deleterious plasmids. One of the variants, tRNA$^{Ala}_{GAA(Phe)}$, was deleterious in single copy and overexpression produced no visible colonies on transformation, demonstrating that overexpressing mistranslating tRNA variants exacerbates the negative growth effect. Of the 17 low impact variants tested, 12 significantly decreased median colony size compared to the control. Four of these had mean colony size 50% less than the control (tRNA$^{Ala}_{UCC(Gly)}$, tRNA$^{Ala}_{CAU(Met)}$, tRNA$^{Ala}_{AGU(Thr)}$, tRNA$^{Ala}_{AAA(Phe)}$) and one variant produced transformants that were too small to quantify (tRNA$^{Ala}_{CUG(Gln)}$). These variants likely mistranslate in single copy, but at a low frequency that does not lead to a growth phenotype. In contrast, five tRNA^{Ala} variants showed no statistical impact on colony size, even in high copy number (tRNA$^{Ala}_{GCA(Cys)}$, tRNA$^{Ala}_{UUU(Lys)}$, tRNA$^{Ala}_{CCA(Trp)}$, tRNA$^{Ala}_{AUA(Tyr)}$, and tRNA$^{Ala}_{CUA(Stop)}$).

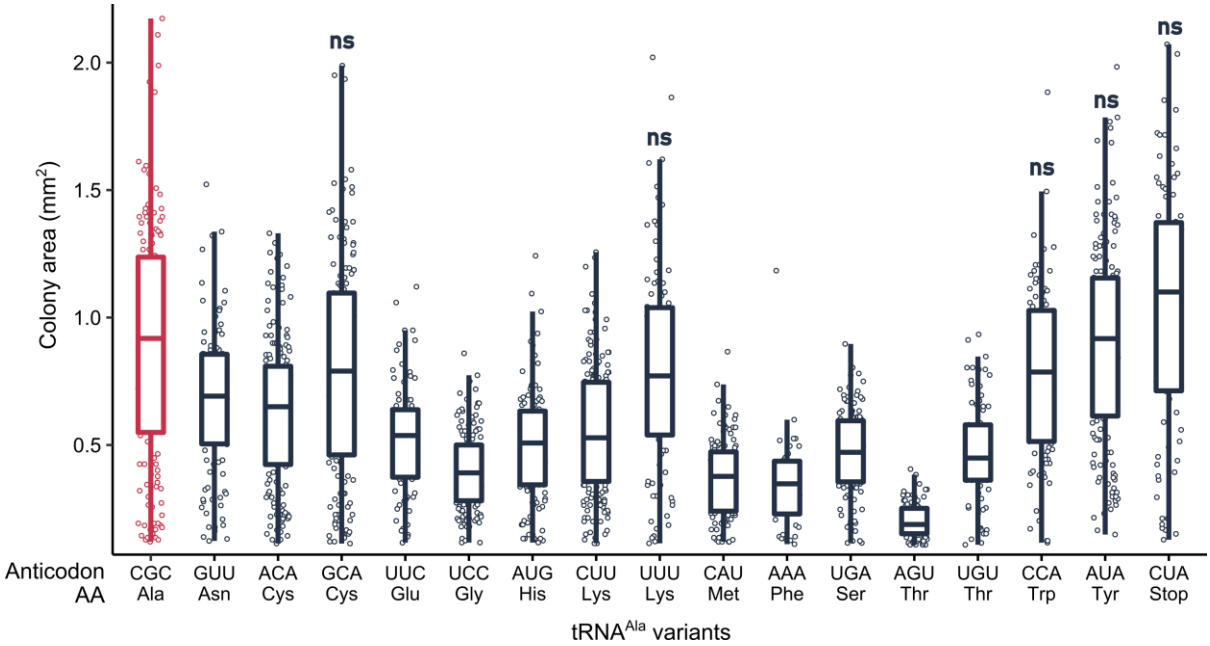

Figure 3. Overexpressing some but not all tRNA^{Ala} variants reduce growth. Strain BY4742 was transformed with 1.0 µg of a *URA3* multicopy plasmid containing each tRNA^{Ala} anticodon variant, plated on medium lacking uracil and grown at 30°C. Transformants were imaged after 48 hrs (raw images are in Figure S3) and colony area was quantified using the ImageJ 'Watershed' package. Each point represents one colony and horizontal bars at the center of each boxplot represent median colony size. Median colony size of each variant was compared to the control tRNA$^{Ala}_{CGC(Ala)}$ (shown in red) using a Wilcoxon rank sum test with Bonferroni correction to determine significance (see Table S8 for *p*-values). All variants are statistically significant ($p < 0.01$) unless denoted by 'ns'.

$tRNA^{Ala}$ anticodon variants mistranslate at different frequencies

Next, we estimated the mistranslation frequency for the $tRNA^{Ala}$ anticodon variants by analyzing the cellular proteome using mass spectrometry after growth of each strain in medium containing 1.0 µg/mL doxycycline. We estimate mistranslation frequency as the ratio of observed unique peptides containing alanine mis-incorporation to the number of observed unique peptides containing the wild-type amino acid (Figure 4A, Table S9). In total, 45 of the 57 non-alanine anticodon variants measured had statistically elevated levels of mistranslated peptides compared to the control strain containing $tRNA^{Ala}_{GGC(Ala)}$ (variants decoding stop codons were not analyzed). Similar to the effect of these variants on growth, we observed a wide range of mistranslation frequencies. For example, $tRNA^{Ala}_{UGG(Pro)}$, $tRNA^{Ala}_{GAC(Val)}$ and $tRNA^{Ala}_{GUG(His)}$ had the highest mistranslation with frequencies of 13.4%, 12.6% and 12.4%, respectively, approximately 40-times above background. Conversely, $tRNA^{Ala}_{AAA(Phe)}$ had the lowest detectable mistranslation at 0.3% (2-times above background).

Many factors may contribute to the frequency with which a tRNA variant mistranslates. These include the presence and number of native tRNA genes that compete to decode a specific codon, stability of codon:anticodon interactions at the ribosome (57), and ribosomal decoding rate of the decoded codon (56). To determine if any of these factors explain the frequency of mistranslation observed for each $tRNA^{Ala}$ variant, we correlated each factor with mistranslation frequency (Figure S4). While there was no correlation between mistranslation frequency and number of competing native tRNAs nor the rate of codon decoding, we found a slight correlation with the strength of codon:anticodon interaction as measured by the Turner binding energetics between codon and anticodon minihelicies (Pearson's $R^2 = 0.15$; $p < 0.005$) (57). As visualized in Figure 4B by Grosjean and Westhof's alternative representation of the genetic code (58), 'weak anticodons' that are A/U rich generally mistranslate at lower frequency compared to 'strong anticodons' that are G/C rich. However, there are exceptions to this trend such as $tRNA^{Ala}_{GAU(Ile)}$, $tRNA^{Ala}_{CAU(Met)}$ and $tRNA^{Ala}_{GAA(Phe)}$, which mistranslate at relatively high frequency. This may be attributed to these tRNA variants being the most G/C rich anticodons of their respective synonymous anticodons, all containing a G or C base at position 34.

In addition to influencing the strength of anticodon:codon pairing, base 34 is often modified and affects decoding specificity (66). Figure 4C shows the mistranslation frequency of synonymous anticodon variants decoding the same amino acid and differing only at position 34. Note only variants with statistically significant levels of mistranslation are shown. For four box anticodons the general order of mistranslation frequency from lowest to highest was U, C, A and G at position 34. The notable exception to this is the proline decoding anticodon UGG, which has the highest mistranslation frequency. As a further indication of reduced mistranslation for variants with U34, no mistranslation was observed for $tRNA^{Ala}_{UCU(Arg)}$, $tRNA^{Ala}_{UAU(Ile)}$, $tRNA^{Ala}_{UUU(Lys)}$ and $tRNA^{Ala}_{UAA(Leu)}$. For the two box anticodons with either G or A at position 34, G34 variants always mistranslated at a greater frequency than the corresponding A34 variant. Our results suggest that $tRNA^{Ala}$ anticodon variants mistranslate at a frequency dependent on the anticodon identity, with G/C rich anticodons mistranslating at a higher frequency than A/U rich anticodons.

Of the 57 possible anticodons not encoding alanine or a stop, 18 are not encoded natively in the *S. cerevisiae* genome. The presence of a Watson-Crick base pairing wild-type competing tRNA may influence the amount of mistranslation for each $tRNA^{Ala}$ variant. However, this is not the case, as shown in Figure 4C, where non-native and native anticodons are represented by empty and filled in points, respectively.

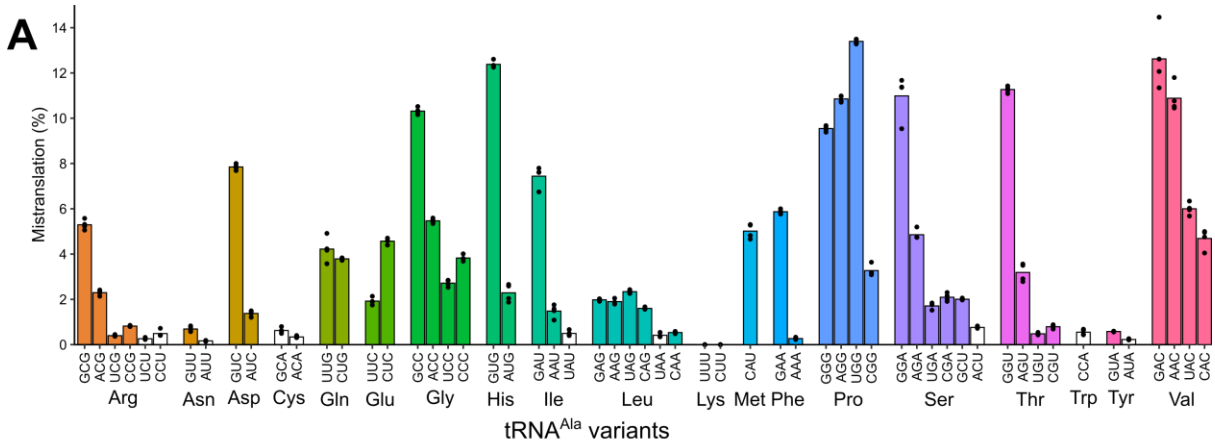
A
Mistranslation (%)
tRNA^Ala variants
Arg
Asn
Asp
Cys
Gln
Glu
Gly
His
Ile
Leu
Lys
Met
Phe
Pro
Ser
Thr
Trp
Tyr
Val

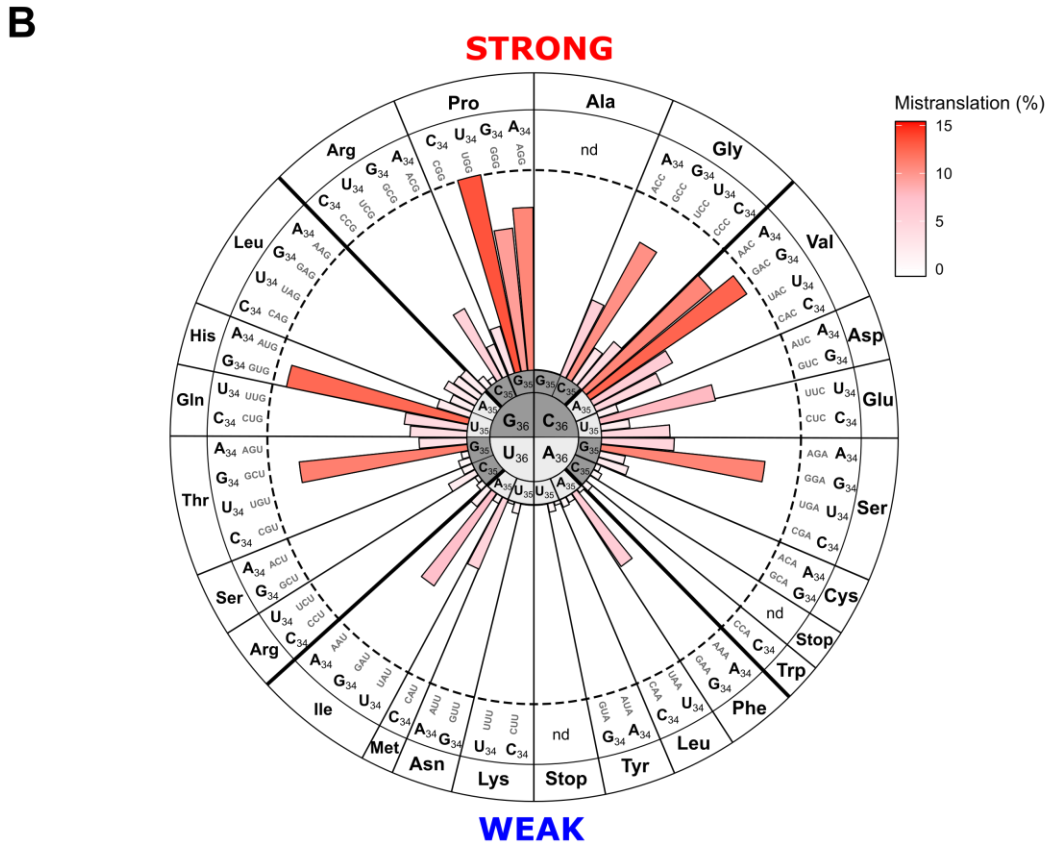
B
STRONG
WEAK
Mistranslation (%)
Pro
Ala
Gly
Val
Asp
Glu
Ser
Cys
Stop
Trp
Phe
Leu
Tyr
Stop
Lys
Asn
Met
Ile
Arg
Ser
Thr
Gln
His
Leu
Arg
nd

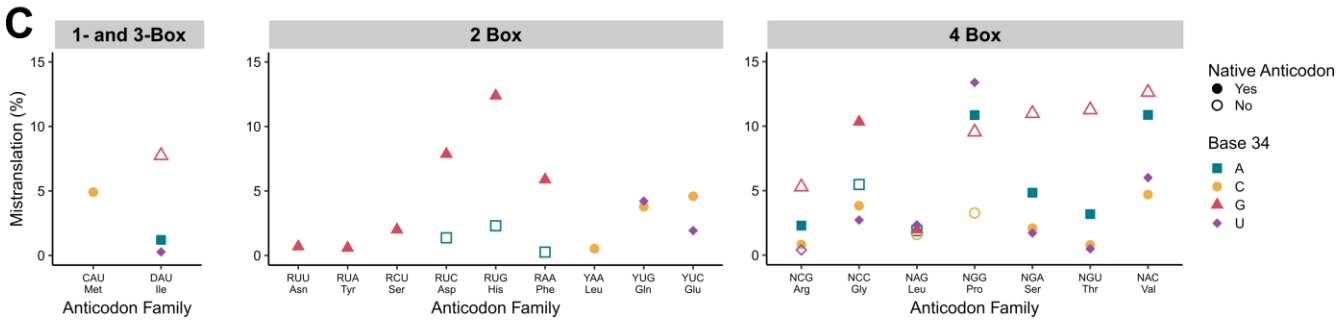
C
1- and 3-Box
2 Box
4 Box
Mistranslation (%)
Anticodon Family
Native Anticodon
Yes
No
Base 34
A
C
G
U

Figure 4. Mistranslation frequency measured by mass spectrometry for $tRNA^{Ala}$ anticodon variants. (A) Yeast strain CY8652 containing either a plasmid with control $tRNA^{Ala}_{GGC(Ala)}$ or a plasmid containing a $tRNA^{Ala}$ anticodon variant were diluted into medium containing 1.0 µg/mL doxycycline to induce tRNA expression and harvested at an OD_{600} of ~ 1.0. Mass spectrometry analysis of the cellular proteome was performed and mistranslation frequency for all variants calculated from the number of unique peptides where alanine mis-incorporation was observed relative to the number of unique peptides where the wild-type amino acid was observed. Each point represents one biological replicate (n ≥ 3). White bars indicate strains where mistranslation is not statistically different from background levels of the same type of mistranslation measured in the control strain (Welch's *t*-test; Benjamini-Hochberg corrected $p < 0.01$). **(B)** Average mistranslation frequency for each $tRNA^{Ala}$ variant as in (A) plotted for each anticodon on Grosjean and Westhof's alternative representation of the genetic code (58) where strong codon:anticodon pairs are at the top of the circle plot and weak pairs are at the bottom. The length of each bar is proportional to the mistranslation frequency. **(C)** Average mistranslation frequency for mistranslating $tRNA^{Ala}$ anticodon variants decoding synonymous anticodons differing in base 34 identity. Only variants with statistically significant levels of mistranslation are shown. Variants are grouped by number of different possible anticodons decoding a specific amino acid (1-, 2-, 3- or 4-box) with the same base at positions 35 and 36. Amino acid identity is listed below the anticodon. Native vs non-native anticodon sequences in yeast are depicted with filled and empty shapes, respectively. D: adenine, guanine or uracil; R: purine; Y: pyrimidine; N: any base.

Factors determining cellular impact of mistranslating $tRNA^{Ala}$ variants

Next, we investigated factors that determine the impact of mistranslating $tRNA^{Ala}$ variants on growth. Previously, we showed that mistranslation frequency correlates with impact on growth when modulating the mistranslation frequency of a serine tRNA variant that mis-incorporates serine at proline codons (17). Other factors that could determine the impact of alanine mis-incorporation include the chemical properties of the substituted amino acid relative to alanine and how many proteins across the proteome will be affected by the mistranslation, as determined by the abundance of each specific codon throughout the genome. To investigate if these factors might correlate with the negative growth impact specific $tRNA^{Ala}$ variants have on cells, we performed multiple linear regression considering five factors: (1) the mistranslation frequency of each variant measured by mass spectrometry; (2) the number of codons in the genome corresponding to each $tRNA^{Ala}$ anticodon; (3) the difference in polarity requirement (PR) value for each replaced amino acid relative to alanine, which describes the biochemical relatedness of each amino acid based on their solubility in pyridine (59); (4) the BLOSUM score for each substitution to alanine, which is based on the evolutionary conservation of amino acids in proteins (60); and (5) the difference in Kyte-Doolittle hydropathy value between each substituted amino acid and alanine (61). Only mistranslation frequency correlated with impact of $tRNA^{Ala}$ variant on growth (Pearson's $R^2 = 0.36$; *p*-value = 6.87×10^{-7}; Figure 5). A similar correlation was observed whether we looked at the absolute number of mistranslation events or the mistranslation frequency observed for each $tRNA^{Ala}$ variant (Figure S5).

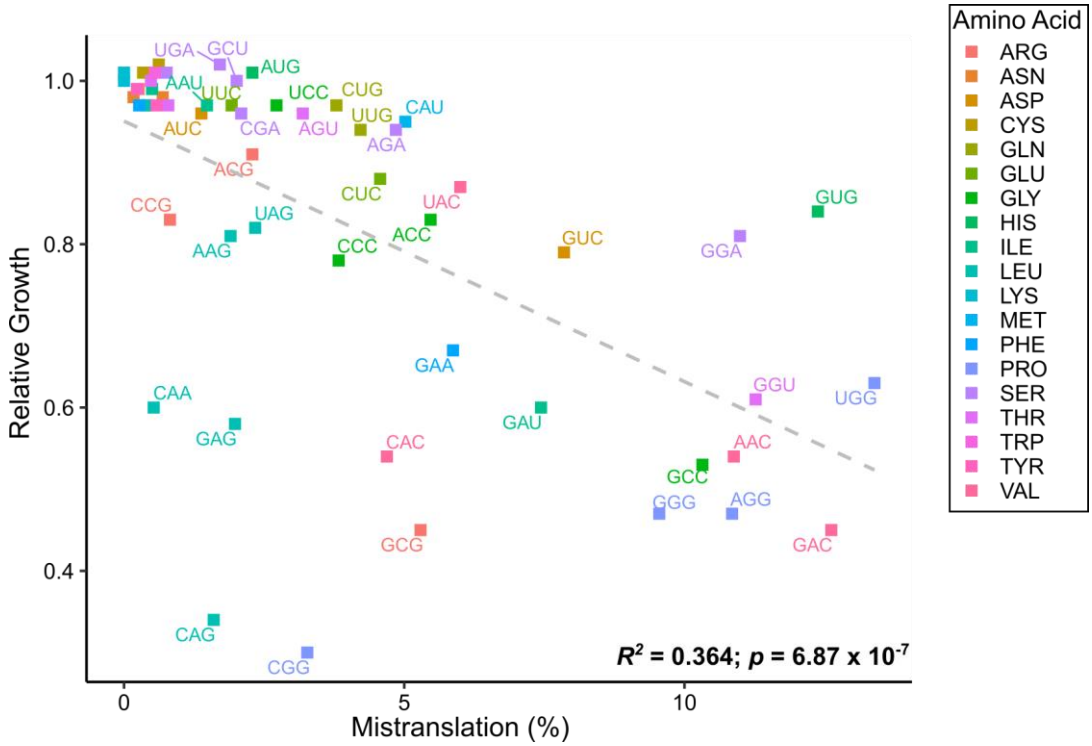

Figure 5. Correlation between mistranslation frequency and impact on growth for tRNA^{Ala} anticodon variants. Relative growth rate for each strain containing a tRNA^{Ala} variant, as calculated in Figure 2A, plotted against the mistranslation frequency determined by mass spectrometry for each tRNA^{Ala} variant, as determined in Figure 4A (for cells grown in medium containing 1.0 µg/mL doxycycline). The grey dashed line represents the correlation between the two variables. The *p*-value is calculated from the linear regression of the dependent variable (percent mistranslation) relative to the independent variable (relative growth).

Although mistranslation frequency and impact on growth correlated, there were several outliers. For example, tRNA$^{Ala}_{CGG(Pro)}$ has the greatest effect on growth but only mistranslates ~3% of proline codons. The other anticodon variants decoding proline (GGG, AGG and UGG) all mistranslate at ~10% and have lesser effects on growth. We hypothesized this difference might be explained by the codon specific mistranslation frequencies for each tRNA^{Ala} variant, as each variant decodes a different subset of codons, which have different usages throughout the transcriptome. The mistranslation frequency for each variant at its cognate and synonymous codons is shown in Figure S6 (see Table S10 for raw values). Indeed, tRNA$^{Ala}_{CGG(Pro)}$ mis-incorporates alanine at 30% of observed CCG codons, whereas variants with AGG, UGG and GGG anticodons mis-incorporate alanine at different subsets of proline codons at lower frequencies (Figure 6A). Further supporting the idea that codon specific mistranslation influences effect on growth, tRNA$^{Ala}_{AGG(Pro)}$ and tRNA$^{Ala}_{GGG(Pro)}$ both mistranslate CCC and CCU codons with similar frequencies and have a similar growth effect.

As another example, tRNA$^{Ala}_{UAC(Val)}$ and tRNA$^{Ala}_{CAC(Val)}$ mistranslate alanine at valine positions with similar frequencies of ~ 5% but their growth is reduced to 87% and 54% of the control strain, respectively. Both tRNA$^{Ala}_{UAC(Val)}$ and tRNA$^{Ala}_{CAC(Val)}$ mistranslate their respective Watson-Crick pairing codons with frequencies of ~15% (Figure 6B), suggesting that codon specific mistranslation frequency was not the main factor leading to the difference in growth impact.

We hypothesized that the difference in growth impact of $tRNA^{Ala}_{UAC(Val)}$ and $tRNA^{Ala}_{CAC(Val)}$ was due to different subsets of the proteome being impacted. In agreement with this, there was minimal overlap in the mistranslated peptides and proteins identified in strains containing these variants (Figure 6C). In contrast, $tRNA^{Ala}_{AAC(Val)}$ and $tRNA^{Ala}_{GAC(Val)}$ both mistranslate at GUU and GUC codons but with different frequencies. These variants mistranslate relatively similar sets of peptides and proteins and their growth impacts were proportional to mistranslation frequency.

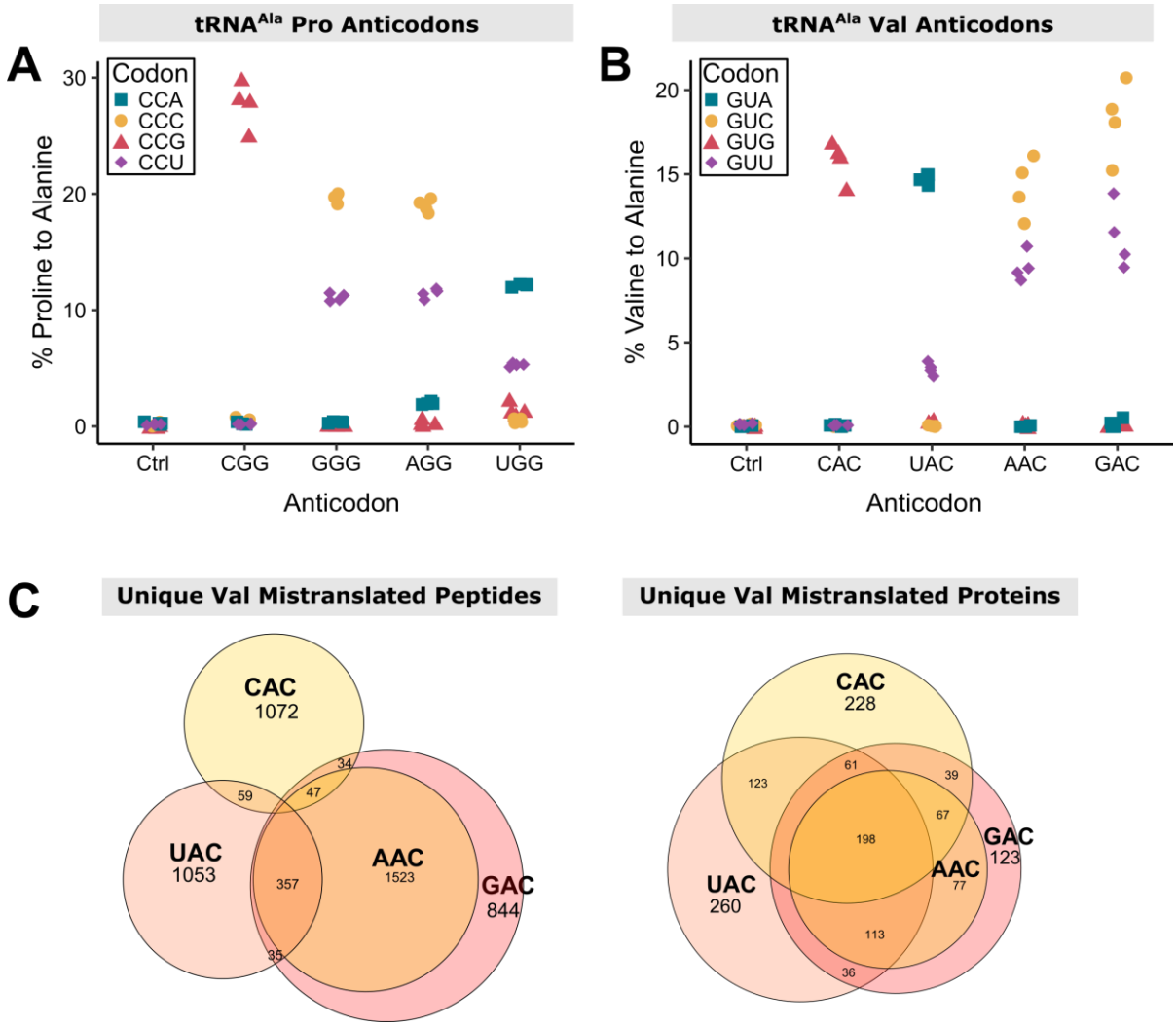

Figure 6. $tRNA^{Ala}$ variants mistranslate at unique codons leading to different subsets of the proteome experiencing mistranslation. (A) Codon specific mistranslation frequencies for the control strain containing $tRNA^{Ala}_{GGC(Ala)}$ and four $tRNA^{Ala}$ variants containing synonymous anticodons decoding proline codons. Mistranslation at each codon was estimated from mass spectrometry data as the ratio of unique mistranslated peptides to wild-type peptides where the proline residue is coded for by the codon indicated. Only peptides containing one proline residue were considered. Each point represents one biological replicate (n = 4). **(B)** Codon specific mistranslation frequencies for the control strain containing $tRNA^{Ala}_{GGC(Ala)}$ and four $tRNA^{Ala}$ variants containing synonymous anticodons decoding valine codons. Codon specific mistranslation was calculated as in (A) only considering peptides containing one valine residue. Each point represents one biological replicate (n = 4). **(C)** Venn diagrams showing the overlap

between the unique peptides (left) and proteins (right) where mistranslation was detected by mass spectrometry in strains containing $tRNA^{Ala}$ variants that have one of four synonymous anticodons decoding valine codons.

To consider the contribution of both the codon specific mistranslation frequency and the subset of the proteome being mistranslated, we calculated a weighted SIFT score for each $tRNA^{Ala}$ variant. This score is the product of the number of possible deleterious substitutions created by each tRNA across the proteome, as predicted by the Sorting Intolerant From Tolerant (SIFT) algorithm (65), multiplied by the amount of mistranslation occurring at each mistranslated codon (Figure 7). When we correlated the weighted SIFT score with growth impact for each variant, there was a similar correlation as that between growth impact and mistranslation frequency (Pearson's $R^2 = 0.41$; $p = 1.87 \times 10^{-7}$); however, we now could identify three groups of variants. Ten variants fall below the line of best fit and thus have a larger impact on growth than predicted by their weighted SIFT score. Included in this group are variants decoding the four proline anticodons (NGG) and three leucine anticodons (CAG, GAG, CAA). Three variants fall above the line, indicating these variants are tolerated better than predicted by their weighted SIFT score ($tRNA^{Ala}_{GAA(Phe)}$, $tRNA^{Ala}_{ACC(Gly)}$, $tRNA^{Ala}_{UAC(Val)}$). The remaining 44 variants fall close to the line of best fit correlating growth impact with weighted SIFT score. Overall, these results suggest that the effect of a mistranslating $tRNA^{Ala}$ variant on growth is dependent on both the number of mistranslation events and the extent to which the specific proteins being targeted are affected.

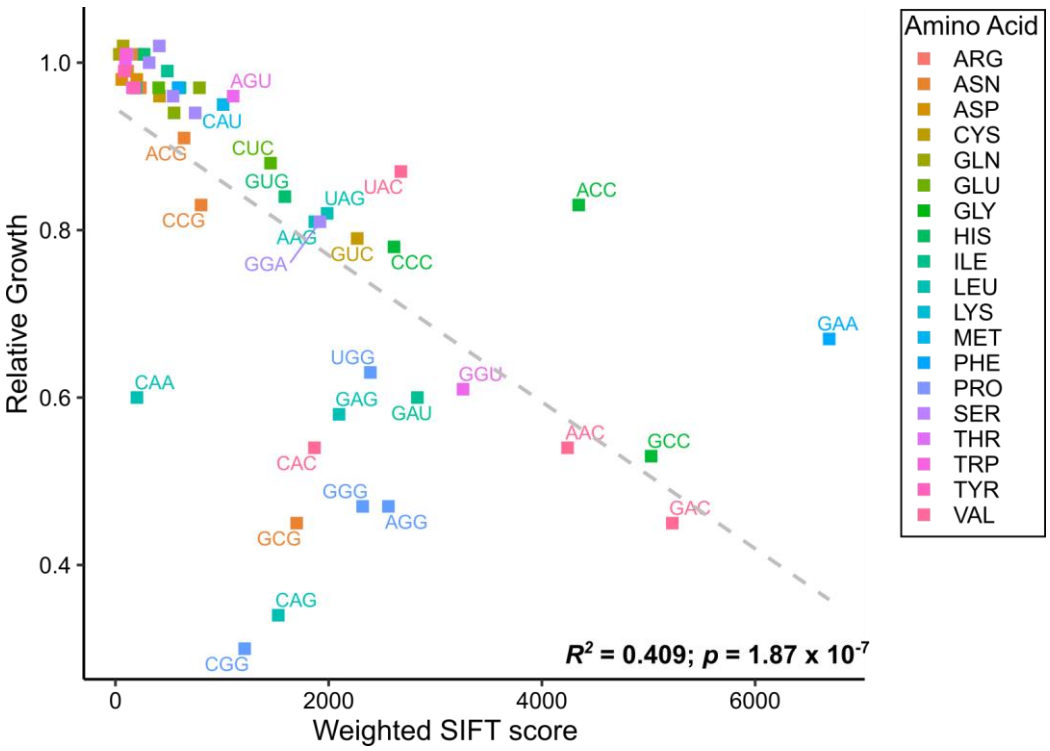

Figure 7. Correlation between weighted SIFT score and impact on growth for tRNA^{Ala} anticodon variants. Relative growth rate for each strain containing a tRNA^{Ala} variant, as calculated in Figure 2A, plotted against their weighted SIFT score which is calculated from the total number of predicted deleterious alanine substitutions at each codon multiplied by the frequency of mistranslation at that codon. The grey dashed line represents the correlation between the two variables. The *p*-value is calculated from the linear regression of the dependent variable (weighted SIFT score) relative to the independent variable (relative growth).

Decoding specificity of the tRNA^{Ala} variants

Figure 8 shows the decoding specificity for variants with statistically elevated mistranslation frequencies. In all but two cases, G at position 34 mistranslates C and the wobble U at the third codon position. Interestingly, in these cases, the majority of mistranslation occurs at C, except in the case of the tRNA$^{Ala}_{GCC(Gly)}$ variant that predominantly decodes GGU codons. Variants with A at position 34 have the potential to be modified to I34 (inosine) and decode codons ending with U, C and A (37, 67, 68). All A34 variants mistranslate codons ending in U and C with the exception of tRNA$^{Ala}_{ACC(Gly)}$. This suggests these variants have expanded decoding consistent with inosine modification; however, we only detected mistranslation at codons ending in A for tRNA$^{Ala}_{AGG(Pro)}$ and tRNA$^{Ala}_{AAG(Leu)}$. Variants with U at position 34 mistranslate at codons ending in A most frequently. We only observed U:G (anticodon:codon) decoding for tRNA$^{Ala}_{UCG(Arg)}$, tRNA$^{Ala}_{UAG(Leu)}$ and tRNA$^{Ala}_{UAC(Val)}$. For tRNA$^{Ala}_{UGG(Pro)}$ and tRNA$^{Ala}_{UAC(Val)}$ we also observed U:U decoding. Finally, tRNA^{Ala} variants with C at position 34 only mistranslate codons ending in G.

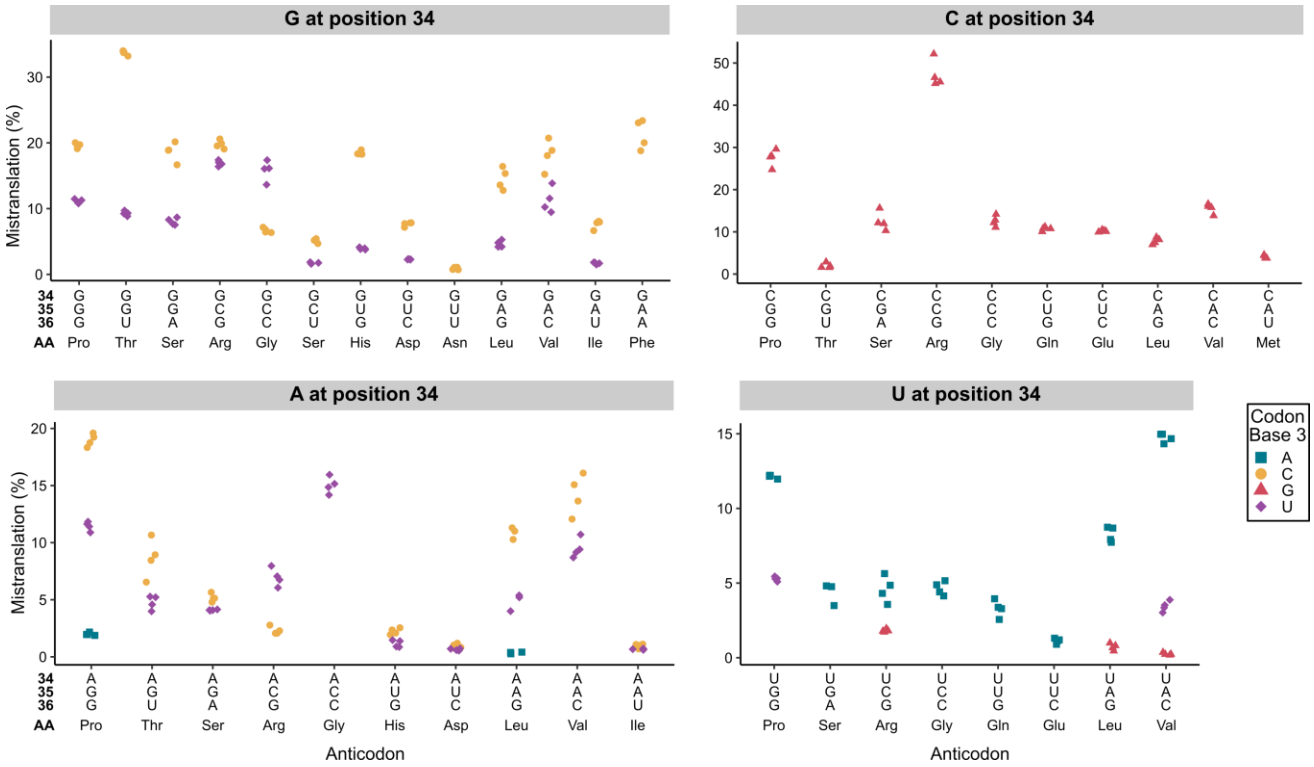

Figure 8. Mistranslation frequency at individual codons for tRNA^{Ala} variants differing at base 34. For each tRNA^{Ala} anticodon variant, mistranslation frequency at each synonymous codon was calculated from the number of unique peptides with a mistranslation event at that codon relative to the number of unique peptides containing a wild-type residue at that specific codon. In all cases, positions 35 and 36 formed Watson-Crick pairs with positions 2 and 1 of the codon, respectively. To confidently localize the mistranslation event and identify the mistranslated codon, only peptides containing a single target amino acid were used in this analysis. Only mistranslation that is statistically above the frequency measured for the same codon in the wild-type strain is shown (Welch's *t*-test; Benjamini-Hochberg corrected $p < 0.01$). Each point represents one biological replicate ($n \geq 3$).

DISCUSSION

Our study characterized the phenotypic impact and mistranslation frequency of the 60 possible $tRNA^{Ala}$ anticodon variants from which three main conclusions could be drawn. First, the impact of a tRNA variant on growth correlates with mistranslation frequency. Second, anticodon sequence is the primary determinant of phenotypic impact and mistranslation potential of $tRNA^{Ala}$ variants. Generally, G/C rich anticodons are the most impactful and U34 anticodons the least impactful. The importance of the anticodon is emphasized by the variable impact of variants decoding synonymous codons. Third, since the extent of mistranslation and characteristics of the amino acid substitution do not fully explain the impact on growth for some variants, we suggest that differences in the specific codons mistranslated by each variant and the subset of proteins that experience mistranslation are significant determinants of phenotypic impact.

Factors determining the mistranslation frequency of $tRNA^{Ala}$ variants

Variants mistranslating at the highest levels have G/C bases at positions 35 and/or 36 with the greatest mistranslation generally seen when an additional G is present at position 34. In contrast, the A/U rich anticodon variants decoding lysine, tyrosine, isoleucine, phenylalanine and asparagine had the lowest mistranslation frequency. We suggest this is because G/C rich anticodons form stronger base pairs that do not require base modifications to stabilize pairing with the mRNA codon in the A site of the ribosome (57, 69). Consistent with this, Pernod *et al.* identified relatively few codon:anticodon interactions between A/U rich codons using an *in vitro* system to investigate decoding interactions (70). tRNAs with A/U rich anticodons are often modified at base 37, 3' of the anticodon, to N^6-isopentenyladenosine or N^6-threonylcarbamoyladenosine to further stabilize base pairing interactions (40). $tRNA^{Ala}$ is modified to 1-methylinosine at A37 (40). Since cognate $tRNA^{Ala}$ anticodons have G35 and C36, it is unlikely this modification stabilizes A/U rich anticodon variants. Thus, base pairing of the A/U rich $tRNA^{Ala}$ variants would not be enhanced in this context, reducing variant mistranslation potential. The finding that U34 generally results in the least mistranslation in sets of synonymous anticodons also highlights the importance of base modification. For each amino acid a U34-containing tRNA isoacceptor exists natively in *S. cerevisiae*. U34 is the site of multiple different modifications depending on the specific native tRNA (38). These modifications are important for fidelity and efficiency of translation and to expand decoding potential (38, 66, 71). If U34 is unmodified or incorrectly modified, translation is impaired. It is possible that in the non-native context of $tRNA^{Ala}$, U34 variants are not modified or modified incorrectly and therefore decode at lower efficiency.

We also considered other factors that could influence mistranslation frequency. Eight non-alanine aaRSs possess editing activity to reduce mischarging (Ile, Leu, Lys, Met, Phe, Ser, Thr, Val) (72). Cross-editing by anticodon-cognate aaRSs could remove alanine from the mischarged $tRNA^{Ala}$ variant (73). However, none of these editing activities are known to target the removal of alanine. Similarly, some $tRNA^{Ala}$ variants may be recognized and aminoacylated by the anticodon-cognate aaRS. If this is the case, a $tRNA^{Ala}$ anticodon variant would be aminoacylated with the amino acid matching its anticodon and no longer result in alanine mis-incorporation. This neutralizing mechanism would be most likely for the 11 aaRSs that use the full anticodon as a primary identity element for aminoacylation (Asn, Asp, Cys, Gln, His, Ile, Lys, Met, Phe, Thr and Trp) (20). Though we cannot rule out this mechanism, there was no difference in the average amount of mistranslation from $tRNA^{Ala}$ anticodon variants where their anticodons are full determinants of aminoacylation by the cognate synthetase compared to variants where their anticodons play a lesser role in aminoacylation (Figure S7). The mistranslation frequency of a $tRNA^{Ala}$ variant would

also be diminished if it was turned over or not expressed. All variants were examined in the same context and importantly, there is no evidence that the anticodon plays a role in the stability of tRNAs (16).

Factors influencing the impact of the tRNA^{Ala} variants on cell growth

Intuitively, we expected a correlation between the growth impact and mistranslation frequency. Previously, we found this was the case when we varied the expression of a single mistranslating tRNA variant and measured mistranslation frequency and growth (74). However, for a set of five different tRNA^{Ser} anticodon variants, Zimmerman *et al.* found that there was not a simple correlation between growth and mistranslation (16). Here, when analyzing the entire set of tRNA^{Ala} variants, the correlation between the extent of mistranslation and the impact on growth was evident but there were many outliers. The general trend suggests that as mistranslation frequency increases, the associated increase in proteotoxic stress slows cell growth. Furthermore, studies in mammalian cells have found that mistranslation results in reduced levels of translation (75), which may also contribute to decreased growth.

We do note that the estimation of mistranslation frequency relies on the detection of mistranslated peptides by mass spectrometry and that the numbers may be an underestimate due to turnover and aggregation of mistranslated proteins. It will be interesting to perform a parallel study in strains with compromised protein quality control pathways to detect mistranslated protein variants that are degraded in wild-type cells.

Since the correlation between mistranslation and growth impact was not exact, we sought other possible mechanisms that might explain the effect of each tRNA^{Ala} variant on growth. Alanine's methyl side chain is small and hydrophobic. Mis-incorporating alanine for amino acids with distinct chemical or functional properties might be expected to have a greater impact on growth. Using several different measures of amino acid similarity, we found no correlation with the impact of each variant on growth. Interestingly, tRNA^{Ala} variants which substitute alanine for similar aliphatic residues such as leucine, isoleucine and valine had significant impacts on growth. Since these aliphatic residues are often embedded in the protein core, their substitution with the smaller alanine may disrupt hydrophobic packing. Supporting this, deep mutational scanning experiments have demonstrated that hydrophobic residues are amongst the most sensitive to substitution (76, 77).

For certain proteins, even small changes in expression or function impact growth (78). Since amino acid and codon composition vary from protein to protein, each tRNA^{Ala} anticodon variant has the potential to contribute to slow growth by decreasing the functional amount of one or more different proteins. The ability of variants to impact distinct cellular pathways is supported by our previous finding where two tRNAs mistranslating alanine at proline codons or serine at arginine codons at similar frequencies had unique sets of genetic interactions (79). Furthermore, because codon usage is not random, synonymous anticodons target different proteins and thus impact growth to different extents. This was seen for tRNA^{Ala} variants with UAC and CAC valine anticodons, which mistranslate at similar frequencies but mis-incorporate alanine into different proteins and have differences in their impact on growth. To take these factors into account, we used SIFT to determine the number of deleterious alanine substitutions for each codon throughout the proteome. After weighting this metric by the mistranslation frequency there was a good correlation with growth impact for the majority of tRNA^{Ala} variants. Of the ten variants with a more severe impact on growth than predicted by the weighted SIFT

scores, seven were proline or leucine anticodons. The reason for this is unclear but could be caused by negative synthetic interactions occurring between multiple mistranslated proteins. Proline may also be an exceptional case because its properties as an imino acid give it unique functionality (80, 81).

Twenty-one $tRNA^{Ala}$ variants mistranslate but do not have an impact on growth. It is likely that for each substitution at a specific codon there is a threshold for the level of proteome-wide mistranslation that is tolerated before growth is impacted. Supporting this, eight of the variants with no effect on growth mistranslate below 1%. Other variants can tolerate higher levels of mistranslation without a growth impact. For example, $tRNA^{Ala}_{CAU(Met)}$ mistranslates at ~5%, the highest frequency we observed without a resulting growth impact. The reason for this is unclear but may in part reflect the relative usage of methionine and the role methionine plays within proteins. Variants decoding stop codons also had minimal impacts on growth. These $tRNA^{Ala}$ anticodons variants likely have the potential to misread stop codons since many stop codon suppressors are tRNAs with altered anticodons (82). The minimal impact of these variants likely results from competition with abundant and efficient translation release factors (83).

In this discussion we have restricted our consideration to the roles of tRNAs in translation. However, many reports are continuing to expand the known roles for tRNAs in other processes. For example, $tRNA^{Gln}_{CUG}$ is important for signaling in response to poor nitrogen sources (84) and the anticodon is required to impart this function (85). We can not exclude the possibility that these non-translational functions contribute to the growth impairment of some of the $tRNA^{Ala}$ variants.

Decoding specificity of anticodon variants

In addition to decoding their Watson-Crick base pair cognate codons, $tRNA^{Ala}$ anticodon variants have the potential to decode near cognate codons through expanded decoding between position 34 of the anticodon and position 3 of the codon. Expanded decoding can occur through G:U wobble pairing or due to modification of base 34. Our dataset allowed us to investigate the *in vivo* decoding specificities for mistranslating $tRNA^{Ala}$ anticodon variants. For most variants with G, C or U at position 34, the Watson-Crick cognate codon was mistranslated the most frequently. Variants with A34 mistranslated codons ending in C and U and to a lesser extent A, consistent with A34 being modified to inosine (67, 86). Only $tRNA^{Ala}_{ACC(Gly)}$, a non-native anticodon, did not show evidence of inosine modification. Interestingly, the fact that A34 containing variants decode codons ending in U more frequently than codons ending in A, despite I:A base pairs being more stable than I:U pairs (87), suggests that there are other factors that modulate inosine base pairing at the ribosome. This could reflect the fact that for two box tRNA families, A34 in the anticodon would result in mistranslation across the box if I:A (anticodon:codon) pairing occurred. It is possible I:A decoding has been minimized in non-cognate circumstances to prevent across the box mistranslation should the A34 mutation arise in the native tRNA. Consistent with this, we did not observe across the box alanine mis-incorporation for two-box anticodon variants with A34.

Anticodon variants with G or U at position 34 also exhibited expanded decoding. For all G34-containing variants except $tRNA^{Ala}_{GUU(Asn)}$ and $tRNA^{Ala}_{GAA(Phe)}$, codons ending in U were mistranslated. Conversely, U34 variants only decoded codons ending in G for three of eight variants. This agrees with previous reports that G:U (anticodon:codon) pairs are more favorable than U:G pairs, unless U is modified (38, 58, 70, 88). For two U34-containing variants ($tRNA^{Ala}_{UGG(Pro)}$ and $tRNA^{Ala}_{UAC(Val)}$), we observed decoding of codons ending in U. In *E. coli* and *Salmonella enterica*, U34 is modified to uridine-5-oxyacetate in $tRNA^{Val}_{UAC}$ and $tRNA^{Pro}_{UGG}$,

respectively, allowing decoding of all four nucleotides in the third codon position (36, 89). In addition, some bacterial and organellar U34 tRNAs 'superwobble', such that an unmodified U34 decodes codons ending in all four nucleotides (90). In *S. cerevisiae*, $tRNA^{Pro}_{UGG}$ is sufficient to decode all four proline codons (91) suggesting that U34 is modified or participates in superwobble. Our data supports a role for expanded decoding by U34 in $tRNA^{Ala}_{UGG(Pro)}$ and $tRNA^{Ala}_{UAC(Val)}$.

Similarities and differences with mistranslating $tRNA^{Ser}$ variants

Previously, Zimmerman *et al.* investigated the growth impact of $tRNA^{Ser}$ variants with all 58 non-serine anticodons in yeast using a competitive growth format (16). While their data was acquired in pooled format, making direct comparison with our $tRNA^{Ala}$ results difficult, their findings of anticodon specific differences including those between synonymous anticodons are consistent with our $tRNA^{Ala}$ results. We previously analyzed some individual $tRNA^{Ser}$ variants (17) and found that in general, $tRNA^{Ser}$ anticodon variants are more toxic than their $tRNA^{Ala}$ counterparts. Differences between $tRNA^{Ala}$ and $tRNA^{Ser}$ variants may arise because modifications are tRNA specific or perhaps because the unique variable arm of $tRNA^{Ser}$ negates interaction with the anticodon cognate aaRSs.

CONCLUSIONS

We have analyzed several factors that contribute to the mistranslation potential of $tRNA^{Ala}$ anticodon variants, with G:C content and base at position 34 being the most important when considering the full set. The extent of mistranslation is a primary determinant of the impact of the variant on cell growth with the specific nature of the amino acid substitution playing a minor role. Furthermore, we suggest that decoding specificity of each variant and the resulting differences in the proteins mistranslated is significant in determining the impact of a mistranslating tRNA.

We and others have predicted that mistranslating tRNA variants act as genetic modifiers of disease by contributing to proteotoxic stress (32, 92, 93). In fact, $tRNA^{Ala}$ variants with altered anticodons are found in the human genome (41). Our work here emphasizes that variant impact will depend on the specific anticodon of a potentially mistranslating tRNA. Our results on the effects of individual anticodon variants may differ somewhat between yeast and humans because of differences in codon usage and buffering tRNAs but strong conservation of the translation process suggests that the same rules will apply. Therefore, our study highlights attributes that may make tRNAs more prone to mistranslation and the factors that contribute to the impact of these variants on cells.

Personalized medicine based upon genetic polymorphism requires the identification of deleterious mutations. Current strategies to characterize the impact of a mutation generally involve comparative analysis of evolutionarily conserved sequences; however, there are limitations to this approach. *In vivo* functional analyses are ideal but given the number of polymorphisms, this is a daunting task using traditional mutagenesis. Extensions of the mistranslation approach used here provide an ideal strategy to analyze the proteome on a global scale.

DATA AVAILABILITY

Raw images and data are available in the supplemental information. The raw mass spectrometry data have been deposited to the ProteomeXchange Consortium via the PRIDE (52) partner repository with the dataset identifier PXD038242 and an annotated list of the file names can be found in Supplemental Table S4.

AUTHOR CONTRIBUTIONS

E.C, C.J.B. and M.D.B conceived and developed the project. E.C. and J.G. cloned the tRNA variants. E.C. conducted the growth experiments, analyzed the data, identified factors correlating with mistranslation frequency and growth impact and created figures 1, 2, 3 and 4 and associated supplemental figures. M.D.B conducted the mass spectrometry experiments with assistance from R.A.R.-M., analyzed the data and created figures 5, 6 and 7 and associated supplemental figures. M.R. constructed multicopy variants. M.R. and M.D. participated in data analysis. C.J.B supervised the work and provided funding. J.V. supervised the mass spectrometry work and provided funding. M.D.B. supervised the project. E.C., C.J.B and M.D.B wrote the manuscript and all authors edited the manuscript.

ACKNOWLEDGMENTS

We would like to thank Josh Isaacson and Josephine Davey-Young for critically reading the manuscript and Tallulah Andrews and members of the Villén lab for insightful discussions.

FUNDING

This work was supported from the Natural Sciences and Engineering Research Council of Canada [RGPIN-2015-04394 to C.J.B.] and generous donations from Graham Wright and James Robertson to M.D.B. Mass spectrometry work was supported by a research grant from the Keck Foundation, National Institutes of Health grants RM1HG010461, R35 GM119536 and associated instrumentation supplement (to J.V.).

Conflict of interest statement. None declared.

REFERENCES

1. Dounce,A.L. (1952) [Duplicating mechanism for peptide chain and nucleic acid synthesis]. *Enzymologia*, **15**, 251–258.

2. Crick,F.H.C., Barnett,L., Brenner,S. and Watts-Tobin,R.J. (1961) General nature of the genetic code for proteins. *Nature*, **192**, 1227–1232.

3. Crick,F. (1970) Central dogma of molecular biology. *Nature*, **227**, 561–563.

4. Nirenberg,M., Leder,P., Bernfield,M., Brimacombe,R., Trupin,J., Rottman,F. and O'Neal,C. (1965) RNA codewords and protein synthesis, VII. On the general nature of the RNA code. *Proc. Natl. Acad. Sci.*, **53**, 1161–1168.

5. Chapeville,F., Lipmann,F., Ehrenstein,G. von, Weisblum,B., Ray,W.J. and Benzer,S. (1962) On the role of soluble ribonucleic acid in coding for amino acids. *Proc. Natl. Acad. Sci.*, **48**, 1086–1092.

6. Ogle,J.M., Murphy,F.V., Tarry,M.J. and Ramakrishnan,V. (2002) Selection of tRNA by the ribosome requires a transition from an open to a closed form. *Cell*, **111**, 721–732.

7. Loveland,A.B., Demo,G., Grigorieff,N. and Korostelev,A.A. (2017) Ensemble cryo-EM elucidates the mechanism of translation fidelity. *Nature*, **546**, 113–117.

8. Loftfield,R.B. and Vanderjagt,D. (1972) The frequency of errors in protein biosynthesis. *Biochem. J.*, **128**, 1353–1356.

9. Stansfield,I., Jones,K.M., Herbert,P., Lewendon,A., Shaw,W.V. and Tuite,M.F. (1998) Missense translation errors in *Saccharomyces cerevisiae*. *J. Mol. Biol.*, **282**, 13–24.

10. Joshi,K., Bhatt,M.J. and Farabaugh,P.J. (2018) Codon-specific effects of tRNA anticodon loop modifications on translational misreading errors in the yeast *Saccharomyces cerevisiae*. *Nucleic Acids Res.*, **46**, 10331–10339.

11. Gomes,A.C., Miranda,I., Silva,R.M., Moura,G.R., Thomas,B., Akoulitchev,A. and Santos,M.A. (2007) A genetic code alteration generates a proteome of high diversity in the human pathogen *Candida albicans*. *Genome Biol.*, **8**, R206.

12. Netzer,N., Goodenbour,J.M., David,A., Dittmar,K.A., Jones,R.B., Schneider,J.R., Boone,D., Eves,E.M., Rosner,M.R., Gibbs,J.S., *et al.* (2009) Innate immune and chemically triggered oxidative stress modifies translational fidelity. *Nature*, **462**, 522–526.

13. Wiltrout,E., Goodenbour,J.M., Fréchin,M. and Pan,T. (2012) Misacylation of tRNA with methionine in *Saccharomyces cerevisiae*. *Nucleic Acids Res.*, **40**, 10494–10506.

14. Lant,J.T., Berg,M.D., Sze,D.H.W., Hoffman,K.S., Akinpelu,I.C., Turk,M.A., Heinemann,I.U., Duennwald,M.L., Brandl,C.J. and O'Donoghue,P. (2018) Visualizing tRNA-dependent mistranslation in human cells. *RNA Biol.*, **15**, 567–575.

15. Santos,M., Pereira,P.M., Varanda,A.S., Carvalho,J., Azevedo,M., Mateus,D.D., Mendes,N., Oliveira,P., Trindade,F., Pinto,M.T., *et al.* (2018) Codon misreading tRNAs promote tumor growth in mice. *RNA Biol.*, **15**, 773–786.

16. Zimmerman,S.M., Kon,Y., Hauke,A.C., Ruiz,B.Y., Fields,S. and Phizicky,E.M. (2018) Conditional accumulation of toxic tRNAs to cause amino acid misincorporation. *Nucleic Acids Res.*, **46**, 7831–7843.

17. Berg,M.D., Zhu,Y., Genereaux,J., Ruiz,B.Y., Rodriguez-Mias,R.A., Allan,T., Bahcheli,A., Villén,J. and Brandl,C.J. (2019) Modulating mistranslation potential of $tRNA^{Ser}$ in *Saccharomyces cerevisiae*. *Genetics*, **213**, 849–863.

18. Rich,A. and RajBhandary,U.L. (1976) Transfer RNA: molecular structure, sequence, and properties. *Annu. Rev. Biochem.*, **45**, 805–860.

19. de Duve,C. (1988) The second genetic code. *Nature*, **333**, 117–118.

20. Giegé,R., Sissler,M. and Florentz,C. (1998) Universal rules and idiosyncratic features in tRNA identity. *Nucleic Acids Res.*, **26**, 5017–5035.

21. Hou,Y.M. and Schimmel,P. (1988) A simple structural feature is a major determinant of the identity of a transfer RNA. *Nature*, **333**, 140–145.

22. Hou,Y.M. and Schimmel,P. (1989) Evidence that a major determinant for the identity of a transfer RNA is conserved in evolution. *Biochemistry*, **28**, 6800–6804.

23. Imura,N., Weiss,G.B. and Chambers,R.W. (1969) Reconstitution of alanine acceptor activity from fragments of yeast $tRNA^{Ala}_{II}$. *Nature*, **222**, 1147–1148.

24. Asahara,H., Himeno,H., Tamura,K., Nameki,N., Hasegawa,T. and Shimizu,M. (1994) *Escherichia coli* seryl-tRNA synthetase recognizes $tRNA^{Ser}$ by its characteristics tertiary structure. *J. Mol. Biol.*, **236**, 738–748.

25. Biou,V., Yaremchuk,A., Tukalo,M. and Cusack,S. (1994) The 2.9 Å crystal structure of *T. thermophilus* seryl-tRNA synthetase complexed with $tRNA^{Ser}$. *Science*, **263**, 1404–1410.

26. Himeno,H., Yoshida,S., Soma,A. and Nishikawa,K. (1997) Only one nucleotide insertion to the long variable arm confers an efficient serine acceptor activity upon *Saccharomyces cerevisiae* $tRNA^{Leu}$ *in vitro*. *J. Mol. Biol.*, **268**, 704–711.

27. Berg,M.D., Hoffman,K.S., Genereaux,J., Mian,S., Trussler,R.S., Haniford,D.B., O'Donoghue,P. and Brandl,C.J. (2017) Evolving mistranslating tRNAs through a phenotypically ambivalent intermediate in *Saccharomyces cerevisiae*. *Genetics*, **206**, 1865–1879.

28. Geslain,R., Cubells,L., Bori-Sanz,T., Álvarez-Medina,R., Rossell,D., Martí,E. and de Pouplana,L.R. (2010) Chimeric tRNAs as tools to induce proteome damage and identify components of stress responses. *Nucleic Acids Res.*, **38**, e30.

29. Francklyn,C. and Schimmel,P. (1989) Aminoacylation of RNA minihelices with alanine. *Nature*, **337**, 478–481.

30. McClain,W.H. and Foss,K. (1988) Changing the identity of a tRNA by introducing a G-U wobble pair near the 3' acceptor end. *Science*, **240**, 793–796.

31. Hoffman,K.S., Berg,M.D., Shilton,B.H., Brandl,C.J. and O'Donoghue,P. (2017) Genetic selection for mistranslation rescues a defective co-chaperone in yeast. *Nucleic Acids Res.*, **45**, 3407–3421.

32. Hoffman,K.S., O'Donoghue,P. and Brandl,C.J. (2017) Mistranslation: from adaptations to applications. *Biochim. Biophys. Acta BBA - Gen. Subj.*, **1861**, 3070–3080.

33. Ruan,B., Palioura,S., Sabina,J., Marvin-Guy,L., Kochhar,S., LaRossa,R.A. and Söll,D. (2008) Quality control despite mistranslation caused by an ambiguous genetic code. *Proc. Natl. Acad. Sci.*, **105**, 16502–16507.

34. Berg,M.D., Isaacson,J.R., Cozma,E., Genereaux,J., Lajoie,P., Villén,J. and Brandl,C.J. (2021) Regulating expression of mistranslating tRNAs by readthrough RNA polymerase II transcription. *ACS Synth. Biol.*, **10**, 3177–3189.

35. Agris,P.F., Vendeix,F.A.P. and Graham,W.D. (2007) tRNA's wobble decoding of the genome: 40 years of modification. *J. Mol. Biol.*, **366**, 1–13.

36. Weixlbaumer,A., Murphy,F.V., Dziergowska,A., Malkiewicz,A., Vendeix,F.A.P., Agris,P.F. and Ramakrishnan,V. (2007) Mechanism for expanding the decoding capacity of transfer RNAs by modification of uridines. *Nat. Struct. Mol. Biol.*, **14**, 498–502.

37. Senger,B., Auxilien,S., Englisch,U., Cramer,F. and Fasiolo,F. (1997) The modified wobble base inosine in yeast $tRNA^{Ile}$ is a positive determinant for aminoacylation by isoleucyl-tRNA synthetase. *Biochemistry*, **36**, 8269–8275.

38. Johansson,M.J.O., Esberg,A., Huang,B., Björk,G.R. and Byström,A.S. (2008) Eukaryotic wobble uridine modifications promote a functionally redundant decoding system. *Mol. Cell. Biol.*, **28**, 3301–3312.

39. Schaffrath,R. and Leidel,S.A. (2017) Wobble uridine modifications-a reason to live, a reason to die?! *RNA Biol.*, **14**, 1209–1222.

40. Boccaletto,P., Machnicka,M.A., Purta,E., Piątkowski,P., Bagiński,B., Wirecki,T.K., de Crécy-Lagard,V., Ross,R., Limbach,P.A., Kotter,A., *et al.* (2018) MODOMICS: a database of RNA modification pathways. 2017 update. *Nucleic Acids Res.*, **46**, D303–D307.

41. Berg,M.D., Giguere,D.J., Dron,J.S., Lant,J.T., Genereaux,J., Liao,C., Wang,J., Robinson,J.F., Gloor,G.B., Hegele,R.A., *et al.* (2019) Targeted sequencing reveals expanded genetic diversity of human transfer RNAs. *RNA Biol.*, **16**, 1574–1585.

42. Woese,C.R. (1965) On the evolution of the genetic code. *Proc. Natl. Acad. Sci. U. S. A.*, **54**, 1546–1552.

43. Rodriguez-Mias,R.A., Hess,K.N., Ruiz,B.Y., Smith,I.R., Barente,A.S., Zimmerman,S.M., Lu,Y.Y., Noble,W.S., Fields,S. and Villén,J. (2022) Proteome-wide identification of amino acid substitutions deleterious for protein function. *bioRxiv*, **doi: 10.1101/2022.04.06.487405**, 9 April 2022, pre-print: not peer-reviewed.

44. Brachmann,C.B., Davies,A., Cost,G.J., Caputo,E., Li,J., Hieter,P. and Boeke,J.D. (1998) Designer deletion strains derived from *Saccharomyces cerevisiae* S288C: a useful set of strains and plasmids for PCR-mediated gene disruption and other applications. *Yeast*, **14**, 115–132.

45. Hughes,T.R., Marton,M.J., Jones,A.R., Roberts,C.J., Stoughton,R., Armour,C.D., Bennett,H.A., Coffey,E., Dai,H., He,Y.D., *et al.* (2000) Functional discovery via a compendium of expression profiles. *Cell*, **102**, 109–126.

46. Berg,M.D., Genereaux,J., Zhu,Y., Mian,S., Gloor,G.B. and Brandl,C.J. (2018) Acceptor stem differences contribute to species-specific use of yeast and human $tRNA^{Ser}$. *Genes*, **9**, E612.

47. Sprouffske,K. and Wagner,A. (2016) Growthcurver: an R package for obtaining interpretable metrics from microbial growth curves. *BMC Bioinformatics*, **17**, 172.

48. Schneider,C.A., Rasband,W.S. and Eliceiri,K.W. (2012) NIH Image to ImageJ: 25 years of image analysis. *Nat. Methods*, **9**, 671–675.

49. Rappsilber,J., Mann,M. and Ishihama,Y. (2007) Protocol for micro-purification, enrichment, pre-fractionation and storage of peptides for proteomics using StageTips. *Nat. Protoc.*, **2**, 1896–1906.

50. Leutert,M., Rodríguez-Mias,R.A., Fukuda,N.K. and Villén,J. (2019) R2-P2 rapid-robotic phosphoproteomics enables multidimensional cell signaling studies. *Mol. Syst. Biol.*, 15: e9021.

51. Eng,J.K., Jahan,T.A. and Hoopmann,M.R. (2013) Comet: an open-source MS/MS sequence database search tool. *Proteomics*, **13**, 22–24.

52. Käll,L., Canterbury,J.D., Weston,J., Noble,W.S. and MacCoss,M.J. (2007) Semi-supervised learning for peptide identification from shotgun proteomics datasets. *Nat. Methods*, **4**, 923–925.

53. Perez-Riverol,Y., Bai,J., Bandla,C., García-Seisdedos,D., Hewapathirana,S., Kamatchinathan,S., Kundu,D.J., Prakash,A., Frericks-Zipper,A., Eisenacher,M., *et al.* (2022) The PRIDE database resources in 2022: a hub for mass spectrometry-based proteomics evidences. *Nucleic Acids Res.*, **50**, D543–D552.

54. Chan,P.P. and Lowe,T.M. (2009) GtRNAdb: a database of transfer RNA genes detected in genomic sequence. *Nucleic Acids Res.*, **37**, D93-97.

55. Chan,P.P. and Lowe,T.M. (2016) GtRNAdb 2.0: an expanded database of transfer RNA genes identified in complete and draft genomes. *Nucleic Acids Res.*, **44**, D184–D189.

56. Gardin,J., Yeasmin,R., Yurovsky,A., Cai,Y., Skiena,S. and Futcher,B. (2014) Measurement of average decoding rates of the 61 sense codons *in vivo*. *eLife*, **3**, e03735.

57. Chen,J.L., Dishler,A.L., Kennedy,S.D., Yildirim,I., Liu,B., Turner,D.H. and Serra,M.J. (2012) Testing the nearest neighbor model for canonical RNA base pairs: revision of GU parameters. *Biochemistry*, **51**, 3508–3522.

58. Grosjean,H. and Westhof,E. (2016) An integrated, structure- and energy-based view of the genetic code. *Nucleic Acids Res.*, **44**, 8020–8040.

59. Woese,C.R., Dugre,D.H., Dugre,S.A., Kondo,M. and Saxinger,W.C. (1966) On the fundamental nature and evolution of the genetic code. *Cold Spring Harb. Symp. Quant. Biol.*, **31**, 723–736.

60. Henikoff,S. and Henikoff,J.G. (1992) Amino acid substitution matrices from protein blocks. *Proc. Natl. Acad. Sci. U. S. A.*, **89**, 10915–10919.

61. Kyte,J. and Doolittle,R.F. (1982) A simple method for displaying the hydropathic character of a protein. *J. Mol. Biol.*, **157**, 105–132.

62. Velculescu,V.E., Zhang,L., Zhou,W., Vogelstein,J., Basrai,M.A., Bassett,D.E., Hieter,P., Vogelstein,B. and Kinzler,K.W. (1997) Characterization of the yeast transcriptome. *Cell*, **88**, 243–251.

63. Stothard,P. (2000) The sequence manipulation suite: JavaScript programs for analyzing and formatting protein and DNA sequences. *BioTechniques*, **28**, 1102, 1104.

64. Wagih,O., Galardini,M., Busby,B.P., Memon,D., Typas,A. and Beltrao,P. (2018) A resource of variant effect predictions of single nucleotide variants in model organisms. *Mol Syst Biol.*, **14**, e8430.

65. Ng,P.C. and Henikoff,S. (2001) Predicting deleterious amino acid substitutions. *Genome Res.,* **11**, 863-874.

66. Agris,P.F., Narendran,A., Sarachan,K., Väre,V.Y.P. and Eruysal,E. (2017) The role of RNA modifications in translational fidelity. *The Enzymes*, **41**, 1–50.

67. Crick,F.H. (1966) Codon--anticodon pairing: the wobble hypothesis. *J. Mol. Biol.*, **19**, 548–555.

68. Torres,A.G., Piñeyro,D., Filonava,L., Stracker,T.H., Batlle,E. and Ribas de Pouplana,L. (2014) A-to-I editing on tRNAs: biochemical, biological and evolutionary implications. *FEBS Lett.*, **588**, 4279–4286.

69. Yarian,C., Townsend,H., Czestkowski,W., Sochacka,E., Malkiewicz,A.J., Guenther,R., Miskiewicz,A. and Agris,P.F. (2002) Accurate translation of the genetic code depends on tRNA modified nucleosides. *J. Biol. Chem.*, **277**, 16391–16395.

70. Pernod,K., Schaeffer,L., Chicher,J., Hok,E., Rick,C., Geslain,R., Eriani,G., Westhof,E., Ryckelynck,M. and Martin,F. (2020) The nature of the purine at position 34 in tRNAs of 4-codon boxes is correlated with nucleotides at positions 32 and 38 to maintain decoding fidelity. *Nucleic Acids Res.*, **48**, 6170–6183.

71. Pereira,M., Francisco,S., Varanda,A.S., Santos,M., Santos,M.A.S. and Soares,A.R. (2018) Impact of tRNA modifications and tRNA-modifying enzymes on proteostasis and human disease. *Int. J. Mol. Sci.*, **19**, 3738.

72. Perona,J.J. and Gruic-Sovulj,I. (2014) Synthetic and editing mechanisms of aminoacyl-tRNA synthetases. *Top. Curr. Chem.*, **344**, 1–41.

73. Ling,J., Reynolds,N. and Ibba,M. (2009) Aminoacyl-tRNA synthesis and translational quality control. *Annu. Rev. Microbiol.*, **63**, 61–78.

74. Berg,M.D., Zhu,Y., Loll-Krippleber,R., San Luis,B.-J., Genereaux,J., Boone,C., Villén,J., Brown,G.W. and Brandl,C.J. (2022) Genetic background and mistranslation frequency determine the impact of mistranslating $tRNA^{Ser}_{UGG}$. *G3 Bethesda*, **12**, jkac125.

75. Lant,J.T., Kiri,R., Duennwald,M.L. and O'Donoghue,P. (2021) Formation and persistence of polyglutamine aggregates in mistranslating cells. *Nucleic Acids Res.*, **49**, 11883–11899.

76. Matreyek,K.A., Starita,L.M., Stephany,J.J., Martin,B., Chiasson,M.A., Gray,V.E., Kircher,M., Khechaduri,A., Dines,J.N., Hause,R.J., *et al.* (2018) Multiplex assessment of protein variant abundance by massively parallel sequencing. *Nat. Genet.*, **50**, 874–882.

77. Gray,V.E., Hause,R.J. and Fowler,D.M. (2017) Analysis of large-scale mutagenesis data to assess the impact of single amino acid substitutions. *Genetics*, **207**, 53–61.

78. Breslow,D.K., Cameron,D.M., Collins,S.R., Schuldiner,M., Stewart-Ornstein,J., Newman,H.W., Braun,S., Madhani,H.D., Krogan,N.J. and Weissman,J.S. (2008) A comprehensive strategy enabling high-resolution functional analysis of the yeast genome. *Nat. Methods*, **5**, 711–718.

79. Berg,M.D., Zhu,Y., Ruiz,B.Y., Loll-Krippleber,R., Isaacson,J., San Luis,B.-J., Genereaux,J., Boone,C., Villén,J., Brown,G.W., *et al.* (2021) The amino acid substitution affects cellular response to mistranslation. *G3 Bethesda*, **11**, jkab218.

80. Deber,C.M., Brodsky,B. and Rath,A. (2010) Proline Residues in Proteins. In John Wiley & Sons, Ltd (ed), *eLS*. Wiley.

81. Melnikov,S., Mailliot,J., Rigger,L., Neuner,S., Shin,B.-S., Yusupova,G., Dever,T.E., Micura,R. and Yusupov,M. (2016) Molecular insights into protein synthesis with proline residues. *EMBO Rep.*, **17**, 1776–1784.

82. Eggertsson,G. and Söll,D. (1988) Transfer ribonucleic acid-mediated suppression of termination codons in *Escherichia coli*. *Microbiol. Rev.*, **52**, 354–374.

83. Albers,S., Beckert,B., Matthies,M.C., Mandava,C.S., Schuster,R., Seuring,C., Riedner,M., Sanyal,S., Torda,A.E., Wilson,D.N., *et al.* (2021) Repurposing tRNAs for nonsense suppression. *Nat. Commun.*, **12**, 3850.

84. Murray,L.E., Rowley,N., Dawes,I.W., Johnston,G.C. and Singer,R.A. (1998) A yeast glutamine tRNA signals nitrogen status for regulation of dimorphic growth and sporulation. *Proc. Natl. Acad. Sci. U. S. A.*, **95**, 8619–8624.

85. Tate,J.J., Rai,R. and Cooper,T.G. (2015) Nitrogen starvation and TorC1 inhibition differentially affect nuclear localization of the Gln3 and Gat1 transcription factors through the rare glutamine $tRNA_{CUG}$ in *Saccharomyces cerevisiae*. *Genetics*, **199**, 455–474.

86. Basilio,C., Wahba,A.J., Lengyel,P., Speyer,J.F. and Ochoa,S. (1962) Synthetic polynucleotides and the amino acid code. V. *Proc. Natl. Acad. Sci. U. S. A.*, **48**, 613–616.

87. Martin,F.H., Castro,M.M., Aboul-ela,F. and Tinoco,I. (1985) Base pairing involving deoxyinosine: implications for probe design. *Nucleic Acids Res.*, **13**, 8927–8938.

88. Rozov,A., Westhof,E., Yusupov,M. and Yusupova,G. (2016) The ribosome prohibits the G•U wobble geometry at the first position of the codon-anticodon helix. *Nucleic Acids Res.*, **44**, 6434–6441.

89. Nasvall,S.J., Chen,P. and Bjork,G.R. (2004) The modified wobble nucleoside uridine-5-oxyacetic acid in $tRNA^{Pro}_{cmo5UGG}$ promotes reading of all four proline codons *in vivo*. *RNA*, **10**, 1662–1673.

90. Rogalski,M., Karcher,D. and Bock,R. (2008) Superwobbling facilitates translation with reduced tRNA sets. *Nat. Struct. Mol. Biol.*, **15**, 192–198.

91. Bloom-Ackermann,Z., Navon,S., Gingold,H., Towers,R., Pilpel,Y. and Dahan,O. (2014) A comprehensive tRNA deletion library unravels the genetic architecture of the tRNA pool. *PLoS Genet.*, **10**, e1004084.

92. Lant,J.T., Berg,M.D., Heinemann,I.U., Brandl,C.J. and O'Donoghue,P. (2019) Pathways to disease from natural variations in human cytoplasmic tRNAs. *J. Biol. Chem.*, **294**, 5294–5308.

93. Reverendo,M., Soares,A.R., Pereira,P.M., Carreto,L., Ferreira,V., Gatti,E., Pierre,P., Moura,G.R. and Santos,M.A. (2014) TRNA mutations that affect decoding fidelity deregulate development and the proteostasis network in zebrafish. *RNA Biol.*, **11**, 1199–1213.